Biofuel Research Journal 47 (2025) 2470-2486

Biofuel Research Journal

Journal homepage: www.biofueljournal.com

Original Research Paper

Microbial photoproduction of *n*-heptane

Ángel Baca-Porcel[1], Poutoum Palakiyém Samire[1], Bertrand Legeret[1], Pascaline Auroy-Tarrago[1], Florian Veillet[1], Cécile Giacalone[1], Stéphan Cuine[1], Solène Moulin[1], Gilles Peltier[1], Yonghua Li-Beisson[1], Fred Beisson[1], Damien Sorigué[1,2,*]

[1]*Aix-Marseille University, CEA, CNRS, Institute of Biosciences and Biotechnologies, BIAM Cadarache, 13108 Saint-Paul-lez-Durance, France.*
[2]*Department of Chemistry, Princeton University, Princeton, New Jersey 08544, United States.*

HIGHLIGHTS

- Co-cultivation boosted microbial *n*-heptane production 14-fold versus co-expression.
- *Cv*FAP fused to Thioredoxin A enhanced hydrocarbon synthesis activity 12-fold.
- 272 mg·L^{-1} *n*-heptane produced within 56 h in 100-mL photobioreactor conditions.
- Blue light-inducible promoter achieved efficient enzyme expression without IPTG.
- High purity (>90%) bio-based *n*-heptane recovery confirmed by GC-MS analysis.

GRAPHICAL ABSTRACT

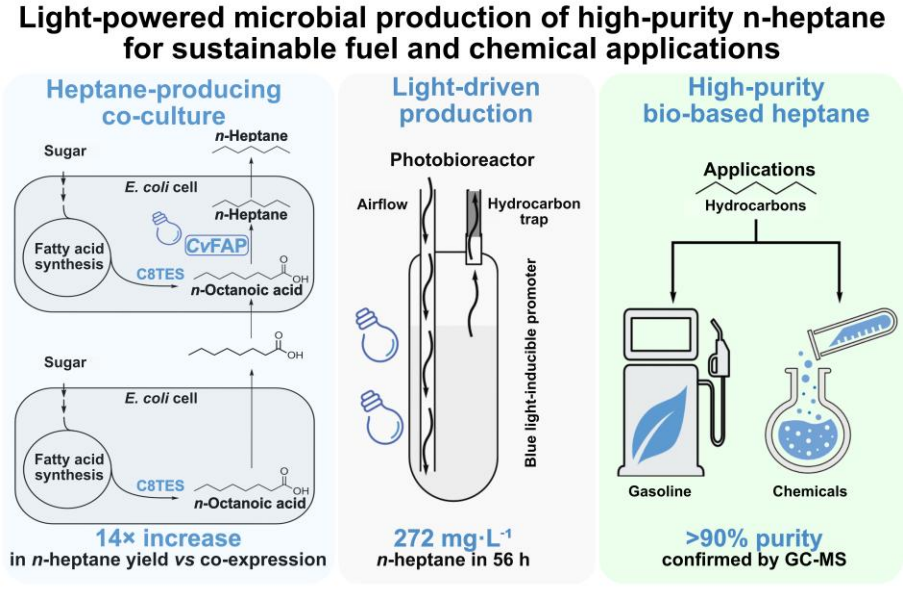

ARTICLE INFO

Article history:
Received 19 April 2025
Received in revised form 15 July 2025
Accepted 27 July 2025
Published 1 September 2025

Keywords:
Drop-in biofuel
Metabolic engineering
Photobiocatalysis
Hydrocarbon production
Co-cultivation strategy
Fatty acid photodecarboxylase

ABSTRACT

The photoenzyme fatty acid photodecarboxylase (FAP) has emerged as a promising catalyst for the redox-neutral biological production of hydrocarbons. Previous studies have shown that FAP can efficiently convert medium-chain fatty acids such as *n*-octanoic acid into hydrocarbons, outperforming its natural long-chain fatty acid substrates (C16-C18). Such observation expands the potential applications of FAP to include solvents and jet fuels. However, the limited availability of natural sources of *n*-octanoic acid poses a challenge to the industrial implementation of *n*-heptane bioproduction. This study investigates the hydrocarbon synthesis capacity of an *E. coli* strain that expresses FAP and produces *n*-octanoic acid, the precursor to *n*-heptane, *via* a specific octanoyl-ACP thioesterase. Several FAPs and thioesterases were tested. A blue light-inducible promoter ensured high expression of both enzymes, eliminating the need for chemical inducers. Fusion of FAP with thioredoxin increased *n*-heptane production 12-fold. Using a co-cultivation strategy, where one strain produces *n*-octanoic acid and another strain converts it to *n*-heptane, increased hydrocarbon production 14-fold compared to co-expressing FAP and thioesterase. Co-cultures operated in batch mode in 100-mL photobioreactors enabled the recovery of >90%-pure *n*-heptane, yielding 272 mg·L^{-1} over 56 h. This work lays the foundation for the development of an industrial bioproduction of *n*-heptane.

* Corresponding author at:
E-mail address: damien.sorigue@cea.fr

Please cite this article as: Baca-Porcel Á., Samire P.P., Legeret B., Auroy-Tarrago P., Veillet F., Giacalone C., Cuine S., Moulin S., Peltier G., Li-Beisson Y., Beisson F., Sorigué D. Microbial photoproduction of *n*-heptane. Biofuel Research Journal 47 (2025) 2470-2486. DOI: 10.18331/BRJ2025.12.3.3.

Contents

Abbreviations

*At*TES	*Anaerococcus tetradius* Thioesterase
BL21(DE3)	*Escherichia coli* strain used for protein expression
C8TES	Octanoyl-ACP Thioesterase
*Ch*TES	*Cuphea hookeriana* Thioesterase
*Cp*TES-287	*Cuphea palustris* Thioesterase variant
*Cv*FAP	*Chlorella variabilis* fatty acid photodecarboxylase
E. coli	*Escherichia coli*
FAD	Flavin Adenine Dinucleotide
FAME	Fatty Acid Methyl Ester
FAP	Fatty acid photodecarboxylase
FID	Flame Ionization Detector
GC-MS	Gas Chromatography - Mass Spectrometry
HCs	Hydrocarbons
IPTG	Isopropyl β-D-1-thiogalactopyranoside
LB	Luria-Bertani
LED	Light-Emitting Diode
MIMS	Membrane Inlet Mass Spectrometry
OD600	Optical Density at 600 nm
pDawn	Light-inducible plasmid and promoter used for gene expression
SDS-PAGE	Sodium Dodecyl Sulfate–Polyacrylamide Gel Electrophoresis
T7	IPTG-inducible promoter system
TB	Terrific Broth
TEV	Tobacco Etch Virus protease
TrxA	Thioredoxin A

1. Introduction

In addition to serving as fuel, hydrocarbons (HCs) derived from petroleum are used as a precursor for a variety of chemicals and have applications in solvents, manufacturing, and cosmetic formulations (Niederer et al., 2016; Kuppusamy et al., 2019). The escalating global demand for fossil HCs, coupled with environmental concerns arising from their exploitation and impending shortages, underscores the urgent need to identify sustainable alternative sources of HCs, especially for use in aviation and chemistry.

Chemical methods of HCs synthesis, such as the Fischer-Tropsch process (Smagala et al., 2013; Teimouri et al. 2021), Kolbe electrolysis (Klüh et al. 2021), and catalytic hydrotreatment of oils (Vignesh et al., 2021; Gil et al. 2024) have been developed to reduce dependence on fossil fuels. While these alternatives are promising, Fischer-Tropsch and Kolbe electrolysis are energy-intensive and only become truly low-carbon when renewable electricity and hydrogen are used. They also involve environmentally unfriendly conditions, such as high temperatures and pressures, as well as the use of polluting metal catalysts. The enzyme-catalyzed synthesis of HCs offers a greener alternative because enzymes typically perform reactions at room temperature and atmospheric pressure, requiring only the energy needed for mixing. Moreover, enzymes are biodegradable, and chemio-, regio-, and stereoselective, thereby limiting waste. Additionally, biocatalysis is safer and limits the use of metal catalysts and solvents. In this context, harnessing the biological synthesis of HCs by industrial microorganisms is a promising biotechnological opportunity (Geng et al., 2023). Although it is still in its early stages compared to conventional industrial processes, it is steadily progressing toward viable and sustainable fuel production.

Remarkably, nature provides a diverse array of organisms, such as plants, insects, bacteria, and microalgae, that possess enzymes capable of converting fatty acids or their derivatives into linear alkanes or alkenes (Lee and Suh, 2013; Herman and Zhang, 2016; Jiménez-Díaz et al., 2017; Jaroensuk et al., 2020). These enzymes have been expressed in yeasts, bacteria, and microalgae to produce HCs (Jiménez-Díaz et al., 2017; Jaroensuk et al., 2020; Geng et al., 2023). Studies employing various enzymes and host strains (Schirmer et al., 2010; Cao et al., 2016; Crépin et al., 2016 and 2018; Fatma et al., 2018; Yunus et al., 2018 and 2022; Bruder et al., 2019; Yang et al., 2019; Amer et al., 2020a and b; Li et al., 2020) have mainly focused on short-chain HCs (e.g., propane, butane, and isobutane) as well as long-chain HCs. The production of medium-chain HCs (C7-C13), which are the major components of gasoline, jet fuel, and solvents (Kuppusamy et al., 2019), was also explored (Akhtar et al., 2013; Blazeck et al., 2013; Rui et al., 2015; Yan et al., 2016; Yunus et al., 2018 and 2022; Moulin et al., 2019). This process involves combining the expression of an HC-forming enzyme with a specific acyl carrier protein thioesterase that shortens fatty acids. However, the yield was limited, and the saturated medium-chain HC was not always the main product.

Fatty acid photodecarboxylase (FAP, EC 4.1.1.106) is the most recently discovered HC-forming enzyme. It catalyzes the flavin-based photodecarboxylation of fatty acids into HCs in algae within the photon wavelength range of 350 to 530 nm (Sorigué et al., 2017). The activity of this photoenzyme has been characterized *in vitro* using a variety of fatty

Please cite this article as: Baca-Porcel Á., Samire P.P., Legeret B., Auroy-Tarrago P., Veillet F., Giacalone C., Cuine S., Moulin S., Peltier G., Li-Beisson Y., Beisson F., Sorigué D. Microbial photoproduction of *n*-heptane. Biofuel Research Journal 47 (2025) 2470-2486. DOI: 10.18331/BRJ2025.12.3.3.

acids, either randomly dispersed in bulk or incorporated into organized lipid assemblies (Sorigué et al., 2017; Huijbers et al., 2018; Zhang et al., 2019; Aselmeyer et al., 2021; Samire et al., 2023). A wealth of biophysical and biochemical experiments has revealed its detailed mechanism (Sorigué et al., 2021). FAP was first identified in the green microalga *Chlorella variabilis* NC64A (Sorigué et al., 2017). It was later found to be conserved with the same activity in various other algae (Moulin et al., 2019).

From a biotechnological standpoint, FAP is interesting because it acts directly on fatty acids and requires no electron donor or additional cofactor besides the native flavin adenine dinucleotide (FAD) (Sorigué et al., 2017). Additionally, unlike other fatty acid decarboxylases such as UndA, UndB, and $OleT_{JE}$, the FAP mechanism does not create a terminal double bond in the HC product (Jaroensuk et al., 2020). Thus, FAP has attracted the attention of biotechnologists and chemists. The FAP from *Chlorella variabilis* (*Cv*FAP) and its derivative mutants have been used in laboratories to produce HCs (Yunus et al., 2018 and 2022; Moulin et al., 2019; Chanquia et al., 2022; Li et al., 2023) but also to synthesize high-value chemicals with high yield and enantioselectivity (Zhang et al., 2020; Emmanuel et al., 2023) and to perform deracemization of racemic mixtures (Cheng et al., 2020; Li et al., 2021).

Interest in the biotechnological potential of FAP for producing medium-chain HCs has been recently revived by the demonstration that *Cv*FAP can efficiently synthesize C7 and C9 *n*-alkanes under specific conditions (Samire et al., 2023). As a purified enzyme, *Cv*FAP exhibits greater activity with *n*-octanoic acid (C8:0) than with *n*-hexadecanoic acid (C16:0). This increased activity on *n*-octanoic acid may be partly due to an autocatalytic effect of the *n*-heptane product that improves substrate stabilization. Additionally, faster substrate turnover, which reduces FAD triplet formation, may explain the higher stability of *Cv*FAP observed in the presence of *n*-octanoic acid (Wu et al., 2021). The high *in vitro* conversion efficiency of *n*-octanoic acid to *n*-heptane by *Cv*FAP has also been observed in feeding experiments, where an *E. coli* strain expressing *Cv*FAP converts externally supplied fatty acids. In this context, the conversion rate of *n*-octanoic acid to *n*-heptane exceeds that of *n*-hexadecanoic acid to *n*-pentadecane by more than tenfold (Samire et al., 2023).

The bio-based production of *n*-heptane is interesting not only because of its role in gasoline but also due to its diverse industrial applications. It is used as a thinner in paints and lacquers, as well as in adhesives, care products, and cleaning agents. Additionally, *n*-heptane is used as a solvent and degreasing agent in the metal industry as well as a cleaning agent in offset and letterpress printing (Rossbach et al., 2012). However, the FAP-based bioproduction of *n*-heptane would still be hampered by the lack of an abundant source of *n*-octanoic acid, such as a vegetable oil that is highly enriched in this fatty acid (Jing et al., 2011; Ohlrogge et al., 2018). Thus, the sustainable production of *n*-heptane by microbial systems requires that the microbes produce *n*-octanoic acid. Some plants and bacteria possess medium-chain thioesterases that can preferentially hydrolyze octanoyl-ACP molecules to produce *n*-octanoic acid and ACP (Dehesh et al., 1996; Jing et al., 2011).

This study explores the potential of *E. coli* strains engineered to express *Cv*FAP and a thioesterase that provides the *n*-octanoic acid precursor for producing *n*-heptane. *n*-Heptane biosynthesis pathways remain largely unexplored. Although this compound is of interest to chemical and transport industries, to date, only one publication deals with its microbial production (see **Table 1**, Yunus et al., 2022). Developing a microbial platform for *n*-heptane synthesis could therefore fill a gap in the range of HC chain lengths accessible through bio-based processes. Various FAPs and thioesterases were evaluated using either a co-expression or a co-cultivation strategy. In preparation for practical industrial applications, a light-inducible promoter was employed to eliminate the need for chemical inducers. The production capacity of the most promising combination was subsequently tested in 100-mL photobioreactors. This work provides the first proof-of-concept for a microbial photoproduction process of *n*-heptane, demonstrating its feasibility while also highlighting key challenges for further optimization and scale-up.

2. Materials and Methods

2.1. Plasmid construction and strains used

Synthetic genes for the different FAP and octanoyl-ACP thioesterases (C8TESs) (**Table 2**) were codon-optimized for expression in *E. coli*. The sequence of the synthetic genes is detailed in **Supplementary Information Table S1**. The FAP genes encode the proteins without their predicted chloroplast transit peptide (Moulin et al., 2021). The *Cv*FAP gene was cloned into pLIC03 and pLIC07 using the BsaI restriction site. The main difference between these two constructions is the presence of thioredoxin A (TrxA) in-frame with *Cv*FAP in pLIC07. The other FAP genes were also cloned into the pLIC07 plasmid, as described previously (Sorigué et al., 2017; Moulin et al., 2021). For cloning *Cv*FAP in the light-inducible plasmid and promoter used for gene expression (pDawn) plasmid, the TrxA-*Cv*FAP fragment was amplified by polymerase chain reaction from the pLIC07-*Cv*FAP construct. The product was cloned between HindIII and XhoI restriction sites.

For cloning the different C8TESs from TrxA-*Cv*FAP into the pDawn plasmid, the C8TES coding sequence from *Cuphea hookeriana* Thioesterase (*Ch*TES) was first cloned into the pDawn plasmid between the NheI and NotI restriction sites, creating the pDawn-*Ch*TES plasmid. Secondly, the TrxA-*Cv*FAP coding sequence was cloned into the pDawn-*Ch*TES plasmid between the NheI and XhoI restriction sites, creating the pDawn-*Ch*TES + *Cv*FAP plasmid. For cloning the remaining C8TESs (*Cuphea palustris* Thioesterase variant (*Cp*TES-287) or *Anaerococcus tetradius* Thioesterase (*At*TES)) coding sequences, the pDawn-*Ch*TES + *Cv*FAP and the pDawn-*Ch*TES were digested with NheI and NotI restriction enzymes to remove the *Ch*TES coding sequence and replace it with the *Cp*TES-287 or *At*TES coding sequences (**Supplementary Information Table S2** for primers). For heterologous protein expression, the following *E. coli* strains were used: DH5α, *Escherichia coli* strain used for protein expression (BL21(DE3)), Rosetta™(DE3), Rosetta-gami™(DE3), C41(DE3) and C43(DE3). The different *E. coli* strains also contain pRIL or pRARE2 plasmids to improve protein expression. The details of all strains used in this study are summarized in **Table 3**.

2.2. Culture conditions in shake flasks

E. coli cells were pre-cultured overnight at 37 °C in Luria-Bertani (LB) broth medium containing antibiotics (kanamycin 50 $\mu g \cdot mL^{-1}$ and chloramphenicol 34 $\mu g \cdot mL^{-1}$). The cultures were initiated at an optical density at 600 nm (OD600) of 0.1 in Terrific Broth (TB) medium containing antibiotics. All experiments were performed in triplicate using 100 mL shake flasks containing 30 mL of culture. The cells were grown in an orbital shaker at 37 °C and 200 rpm in the dark. When the OD600 reached ~0.8, the temperature was lowered to 20 °C and protein expression was induced using different concentrations of isopropyl β-D-1-thiogalactopyranoside (IPTG) (0–2 mM) or different intensities of blue-light (0–1.2 µmol photons$\cdot m^{-2} \cdot s^{-1}$) *via* light-emitting diodes (LED). The cultures were grown under these conditions for 16 or 18 h. For experiments involving the addition of *n*-octanoic acid, 300 µL of ethanol containing *n*-octanoic acid (0–8 mM final concentration) was added to the cultures after a 16-h induction period. The cultures were then incubated for 2 h in the dark at 20 °C. Samples were collected for sodium dodecyl sulfate-polyacrylamide gel electrophoresis (SDS-PAGE), immunoblot analysis, and fatty acid analysis using gas chromatography coupled to mass spectrometry (GC-MS) or flame ionization detection (FID) to determine the *n*-heptane production capacity (see below).

A different culture protocol was used in experiments where the strain expressing FAP and the strain producing *n*-octanoic acid were co-cultured or mixed (four conditions in total). For conditions 1 through 3, the strains were pre-cultured separately overnight at 37 °C in LB broth medium containing antibiotics (kanamycin at 50 $\mu g \cdot mL^{-1}$ and chloramphenicol at 34 $\mu g \cdot mL^{-1}$). Then, cultures were inoculated separately at an optical density (OD600) of 0.1 in TB medium with antibiotics. For condition 4, each strain was pre-cultured as described above. Cultures were initiated by inoculating an equal number of cells from each strain into the same flask to reach a final

Please cite this article as: Baca-Porcel Á., Samire P.P., Legeret B., Auroy-Tarrago P., Veillet F., Giacalone C., Cuine S., Moulin S., Peltier G., Li-Beisson Y., Beisson F., Sorigué D. Microbial photoproduction of *n*-heptane. Biofuel Research Journal 47 (2025) 2470-2486. DOI: 10.18331/BRJ2025.12.3.3.

Table 1.
Overview of engineered microbial strains reported for medium-chain HCs production.

Enzymes Modified	Enzyme Source	Host Organism	Metabolic Engineering	HCs	Yield ($mg \cdot L^{-1}$)	Productivity ($mg \cdot L^{-1} \cdot h^{-1}$)
*Cv*FAP *Cp*TES AAS	*Chlorella varialbilis* (*Cv*FAP) *Cuphea palustris* (*Cp*TES)	*Synechocystis* sp. PCC6803	Overexpression of *Cv*FAP and *Cp*TES Deletion of AAS gene	*n*-Heptane *n*-Nonane *n*-Undecane *n*-Tridecane	~9*[a]	~0.036*[a]
*Cv*FAP *Uc*TES AAS	*Chlorella varialbilis* (*Cv*FAP) *Umbellularia californica* (*Uc*TES)	*Synechocystis* sp. PCC6803	Overexpression of *Cv*FAP and *Uc*TES Deletion of AAS gene	*n*-Undecane *n*-Tridecane	26*[a]	~0.11*[a]
UndB *Ch*TES AAS	*Pseudomonas mendocina* (UndB) *Cuphea hookeriana* (*Ch*TES)	*Synechocystis* sp. PCC6803	Overexpression of UndB and *Ch*TES Deletion of AAS gene	1-Heptene 1-Nonene 1-Undecene 1-Tridecene	~5.5*[a]	~0.023*[a]
UndB *Uc*TES AAS	*Pseudomonas mendocina* (UndB) *Umbellularia californica* (*Uc*TES)	*Synechocystis* sp. PCC6803	Overexpression of UndB and *Uc*TES Deletion of AAS gene	1-Undecene 1-Tridecene	257[a]	~1.07*[a]
*Cv*FAP *Uc*TES	*Chlorella varialbilis* (*Cv*FAP) *Umbellularia californica* (*Ch*TES)	*E. coli*	Overexpression of CvFAP and *Uc*TES	*n*-Undecane *n*-Tridecane *n*-Tridecene *n*-Pentadecane *n*-Pentadecene *n*-Heptadecane *n*-Heptadecene	96*[b]	0.8*[b]
UndB *Uc*TES	*Pseudomonas mendocina* (UndB) *Umbellularia californica* (*Uc*TES)	*E. coli*	Overexpression of UndB and *Uc*TES	1-Undecene 1-Tridecene	~63*[c]	~1.313*[c]
FadE FadR FadD 'TesA (L109P) ACR CER1	*E. coli* (FadD and 'TesA(L109P)) *Clostridium acetobutylicum* (ACR) *Arabidopsis thaliana* (CER1)	*E. coli*	Overexpression of TesA(L109P), FadD, ACR, CER1 Deletion of FadE and fadR	*n*-Dodecane *n*-Tridecane 2-methyl-dodecane *n*-Tetradecane	580.8[d]	Unknown[d]

Abbreviations: *Cv*FAP, *Chlorella variabilis* fatty acid photodecarboxylase; *Ch*TES, *Cuphea hookeriana;* octanoyl-ACP/CoA thioesterase; *Cp*TES, *Cuphea palustris* octanoyl-ACP/CoA thioesterase; *Uc*TES, *Umbellularia californica* dodecyl-ACP/CoA thioesterase; AAS, *Synechocystis sp. PCC 6803* acyl-ACP synthetase; UndB, *Pseudomonas mendocina* fatty acid decarboxylase; FadE, *E. coli* acyl-CoA dehydrogenase; FadR, *E. coli* fatty acid metabolism regulator protein; FadD, *E. coli* fatty acyl-CoA synthetase; TesA(L109P), *E. coli* thioesterase A (leaderless and with a L109P mutation), ACR, *Clostridium acetobutylicum* fatty acyl-CoA reductase; CER1, *Arabidopsis thaliana* aldehyde decarbonylase. * Values calculated based on data from the original publications.

[a] Yunus et al. (2022)
[b] Moulin et al. (2019)
[c] Rui et al. (2015)
[d] Choi and Lee (2013)

Table 2.
Fatty acid photodecarboxylases (FAPs) and *n*-Octanoyl-ACP specific thioesterases (C8TESs) used in this study.*

Enzyme	Abbreviation	Source	Accession
Fatty acid photodecarboxylase	*Cv*FAP	*Chlorella variabilis* (Green microalga)	A0A248QE08.1
	*Cr*FAP	*Chlamydomonas reinhardtii* (Green microalga)	XP_001703004
	*Cc*FAP	*Chondrus crispus* (Red macroalga)	XP_005714951
	*Gs*FAP	*Galderia sulphuraria* (Red microalga)	OR839187.1
	*Es*FAP	*Ectocarpus silicolusus* (Brown macroalga)	CBJ25560
	*Ng*FAP	*Nannochloropsis gaditana* (Eustigmatophyte microalga)	OR839186.1
n-Octanoyl-CoA specific thioesterase	*At*TES	*Anaerococcus tetradius* (Bacterium)	WP_004837416.1
	*Cp*TES-287	*Cuphea palustris* (Plant)	AAC49179.1
	*Ch*TES	*Cuphea hookeriana* (Plant)	AAC49269.1

* The *Cp*TES-287 variant was derived from *Cp*FatB1.2-M4–287 (Hernández Lozada et al., 2018) and includes an N-terminal truncation of 112 residues and two mutations (N122S and I159M). The *Ch*TES variant corresponds to *Ch*FatB2 (Dehesh et al., 1996).

Please cite this article as: Baca-Porcel Á., Samire P.P., Legeret B., Auroy-Tarrago P., Veillet F., Giacalone C., Cuine S., Moulin S., Peltier G., Li-Beisson Y., Beisson F., Sorigué D. Microbial photoproduction of *n*-heptane. Biofuel Research Journal 47 (2025) 2470-2486. DOI: 10.18331/BRJ2025.12.3.3.

Table 3.
E. coli strains used in this work.

***E. coli* strain name**	**Genetic background**	**Relevant Genotype**	**Ref.**
BL21(DE3)	B834	*E. coli* str. B F^- ompT gal dcm lon $hsdS_B(r_B^-m_B^-)$ λ(DE3 [lacI lacUV5-T7p07 ind1 sam7 nin5]) $[malB^+]_{K-12}(\lambda^S)$	_
Rosetta™(DE3)	BL21(DE3)	F^-ompT $hsdS_B(r_B^- m_B^-)$ gal dcm (DE3) pRARE, Cam^R	_
Rosetta-gami™ 2(DE3)	Rosetta™(DE3)	Δ(ara-leu)7697 ΔlacX74 ΔphoA PvuII phoR araD139 ahpC galE galK rpsL (DE3) F′[lac^+ $lacI^q$ pro] gor522:Tn10 trxB pRARE2 Cam^R, Str^R, Tet^R	_
C41(DE3)	BL21(DE3)	F^- ompT gal dcm $hsdS_B(r_B^- m_B^-)$(DE3)	_
C43 (DE3)	C41(DE3)	F^- ompT hsdSB (rB- mB-) gal dcm (DE3)	_
DH5α	K-12	fhuA2 lac(del)U169 phoA glnV44 Φ80′ lacZ(del)M15 gyrA96 recA1 relA1 endA1 thi-1 hsdR17	_
BL21(DE3) pRIL	BL21(DE3)	pRIL in BL21(DE3), Cam^R	_
BL21(DE3) pRARE2	BL21(DE3)	pRARE2 in BL21(DE3), Cam^R	_
DH5α pRIL	DH5α	pRIL in DH5α, Cam^R	_
BL21(DE3) pRIL pLIC03	BL21(DE3) pRIL	pLIC03 in BL21(DE3) pRIL, Cam^R	_
BL21(DE3) pRIL pLIC03-*Cv*FAP		pLIC03-*Cv*FAP in BL21(DE3) pRIL, Cam^R	**This Study**
BL21(DE3) pRIL pLIC07		pLIC07 in BL21(DE3) pRIL, Cam^R	Sorigué et al. (2017)
BL21(DE3) pRIL pLIC07-*Cv*FAP		pLIC07-*Cv*FAP in BL21(DE3) pRIL, Cam^R	
BL21(DE3) pRIL pLIC07-*Cr*FAP		pLIC07-*Cr*FAP in BL21(DE3) pRIL	Moulin et al. (2021)
BL21(DE3) pRIL pLIC07-*Cc*FAP		pLIC07-*Cc*FAP in BL21(DE3) pRIL	
BL21(DE3) pRIL pLIC07-*Gs*FAP		pLIC07-*Gs*FAP in BL21(DE3) pRIL	
BL21(DE3) pRIL pLIC07-*Es*FAP		pLIC07-*Es*FAP in BL21(DE3) pRIL	
BL21(DE3) pRIL pLIC07-*Ng*FAP		pLIC07-*Ng*FAP in BL21(DE3) pRIL	
BL21(DE3) pRIL pDawn		pDawn in BL21(DE3) pRIL	**This Study**
BL21(DE3) pRIL pDawn-*Cv*FAP		pDawn-*Cv*FAP in BL21(DE3) pRIL	
BL21(DE3) pRIL pDawn-*At*TES+*Cv*FAP		pDawn-*At*TES+*Cv*FAP in BL21(DE3) pRIL	
BL21(DE3) pRIL pDawn-*Cp*TES-287+*Cv*FAP		pDawn-*Cp*TES-287+*Cv*FAP in BL21(DE3) pRIL	
BL21(DE3) pRIL pDawn-*Ch*TES+*Cv*FAP		pDawn-*Ch*TES+*Cv*FAP in BL21(DE3) pRIL	
BL21(DE3) pRIL pDawn-*Ch*TES		pDawn-*Ch*TES in BL21(DE3) pRIL	
BL21(DE3) pRIL pDawn-*Cp*TES-287		pDawn-*Cp*TES-287 in BL21(DE3) pRIL	
BL21(DE3) pRIL pDawn-*At*TES		pDawn-*At*TES in BL21(DE3) pRIL	
BL21(DE3) pRARE2 pDawn-*Ch*TES+*Cv*FAP	BL21(DE3) pRARE2	pDawn-*Ch*TES+*Cv*FAP in BL21(DE3) pRARE2	
Rosetta(DE3)™ pDawn-*Ch*TES+*Cv*FAP	Rosetta™(DE3)	pDawn-*Ch*TES+*Cv*FAP in Rosetta™(DE3)	
Rosetta-gami™ 2(DE3) pDawn-*Ch*TES+*Cv*FAP	Rosetta-gami™ 2(DE3)	pDawn-*Ch*TES+*Cv*FAP in Rosetta-gami™ 2(DE3)	

Please cite this article as: Baca-Porcel Á., Samire P.P., Legeret B., Auroy-Tarrago P., Veillet F., Giacalone C., Cuine S., Moulin S., Peltier G., Li-Beisson Y., Beisson F., Sorigué D. Microbial photoproduction of *n*-heptane. Biofuel Research Journal 47 (2025) 2470-2486. DOI: 10.18331/BRJ2025.12.3.3.

Table 3.
continued.

E. coli strain name	Genetic background	Relevant Genotype	Ref.
C41(DE3) pRIL pDawn-*Ch*TES+*Cv*FAP	C41(DE3) pRIL	pDawn-*Ch*TES+*Cv*FAP in C41(DE3) pRIL	This Study
C43(DE3) pRIL pDawn-*Ch*TES+*Cv*FAP	C43(DE3) pRIL	pDawn-*Ch*TES+*Cv*FAP in C43(DE3) pRIL	
DH5α pRIL pDawn-*Ch*TES+*Cv*FAP	DH5α pRIL	pDawn-*Ch*TES+*Cv*FAP in DH5α pRIL	

OD600 of 0.1. Cell cultures were performed in triplicate for all conditions using 200-mL shake flasks containing 50 mL of culture. The flasks were agitated at 37 °C in an orbital shaker at 200 rpm in the dark. When the OD600 reached ~0.8, the temperature was reduced to 20 °C, and protein expression was induced by exposure to blue LED light at an intensity of 0.2 µmol photons·m^{-2}·s^{-1}. The cultures were grown under these conditions for 18 h. Then, depending on the experimental condition, different mixtures were performed. For condition 1, a 50-mL culture of the *E. coli* strain expressing *Cv*FAP together with *Ch*TES was centrifuged at 3,200 g for 15 min, and the entire supernatant was discarded. Then, a 50-mL culture of the *E. coli* strain expressing only *Ch*TES was added to the pellet and resuspended. For condition 2, a 50-mL culture of the *E. coli* strain expressing both *Cv*FAP and ChTES was centrifuged at 3,200 g for 15 min, and 25 mL of the supernatant was discarded. Then, a 25-mL culture of the *E. coli* strain expressing only *Ch*TES was added to the remaining 25 mL and mixed. For condition 3, a 25-mL culture of the *E. coli* strain expressing *Cv*FAP and ChTES was mixed with a 25-mL culture of the *E. coli* strain expressing only ChTES. No mixing was performed for condition 4. Then, 5-mL samples were collected for conditions 1 through 4 to determine the *n*-heptane production capacity in 10-mL vials (see *Section 2.4*).

2.3. Analysis of hydrocarbons and fatty acids in cells and culture medium

To quantify the HCs and fatty acids present in cells cultivated in shake flasks, the equivalent of 1 mL of cell culture at an OD600 of 10 was pelleted at 3200 g for 15 min. If the cells had been previously incubated with *n*-octanoic acid, the pellets were washed and centrifuged three times with TB to remove any remaining fatty acids. Then, internal standards (10 µg of *n*-hexadecane and 10 µg of triheptadecanoylglycerol) were added for quantification, and the cell pellets were transmethylated with 1 mL of methanol containing 5% sulfuric acid by heating in sealed glass tubes at 85 °C for 90 min. After cooling, 1.5 mL of 0.9% NaCl and 500 µL of *n*-hexane were added. The samples were shaken for 5 min and then centrifuged at 3,200 g for 5 min to allow phase separation and recovery of the HCs and fatty acid methyl esters (FAMEs) in the organic phase. Finally, the *n*-hexane phase was analyzed by GC-MS/FID.

To quantify *n*-octanoic acid in the culture medium, the cell cultures were centrifuged at 3200 g for 15 min. The supernatant was collected, and the cells were washed three times with fresh culture medium to remove fatty acids present at the cell surface. Then, 50 µL of the pooled supernatant was taken for analysis. An internal standard of 10 µg of *n*-nonanoic acid was added for quantification, and the samples were transmethylated with 2 mL of methanol containing 5% sulfuric acid by heating for 90 min at 85 °C in sealed glass tubes. After cooling, 3 mL of 0.9% NaCl and 500 µL of *n*-hexane were added. The samples were treated as described above: shaken for 5 min and centrifuged at 3,200 g for 5 min to allow phase separation. The *n*-hexane phases containing the FAMEs were analyzed by GC-MS/FID.

2.4. Determination of the n-heptane production capacity in vials

Five mL of cultures from shake flasks were transferred to 10-mL vials, which were hermetically sealed. The vials were then illuminated with 300 µmol photons·m^{-2}·s^{-1} of blue light for between 15 min and 6 h.

In experiments measuring total HC content (cells, media, and gas phase), the vials were heated at 100 °C for 20 min to stop enzymatic reactions and lyse the cells. The vials were then cooled and heated again to 40 °C for 5 min just before headspace gas chromatography-mass spectrometry/flame ionization detector (GC-MS/FID) analysis to release all HCs in the vial's headspace. For experiments measuring volatile HCs released by living cells, the vials were placed in the dark immediately after illumination to stop the reaction. The gas phase was then analyzed using headspace GC-MS/FID.

2.5. Escherichia coli cell viability assays

To assess the toxicity of *n*-octanoic acid *in E. coli*, cells were diluted in a range of concentrations (from 1:10 to 1:108), and 5 µL of the diluted solution was dropped onto LB 15% (w/v) agar plates. The plates were then incubated overnight at 37 °C before observation.

2.6. Sodium dodecyl sulfate–polyacrylamide gel electrophoresis and immunoblot analysis

One mL of the *E. coli* shake flask culture was collected by centrifugation at 11,000 g for 5 min. The pellets were then resuspended in 50 mM Tris buffer at pH 8 and sonicated. The cell lysates were then mixed with 2X NuPAGE™ LDS Sample Buffer and 50 mM dithiothreitol (DTT), after which they were boiled for 20 min at 70 °C. The proteins were loaded on a constant OD600 basis and separated using NuPAGE™ Bis-Tris 10% precast gels in SDS-PAGE. To determine the size of the proteins, a PageRuler™ protein ladder was used, and the proteins were stained with ProSieve™ EX Safe Stain. For immunoblot analysis, the proteins were transferred onto a BioTrace NT nitrocellulose membrane (Sigma-Aldrich). The membrane was blocked with 5% dried milk in Tris-buffered saline containing 0.1% Tween 20 overnight at 4 °C. To detect His-tagged FAP and C8TES proteins, the membrane was incubated at room temperature for 1 h with a rabbit anti-His antibody conjugated with horseradish peroxidase (HRP) (Amersham Biosciences). To detect *Cv*FAP protein in bacterial strains harboring *Cv*FAP and C8TES genes in pDawn plasmids, the membrane was first incubated with specific polyclonal rabbit primary antibodies (dilution 1:2000) for 1 h. Then, it was incubated with a secondary anti-rabbit antibody coupled to HRP (Amersham Biosciences) for 1 h. Immobilon™ Western Chemiluminescent HRP substrate (EMD Millipore) was used for detection. Images were recorded using a G:BOX Chemi XL (Syngene).

2.7. Fatty acid photodecarboxylase production and purification

All purification steps were carried out under red light to minimize the inhibition of FAP by light. Recombinant *Cv*FAP and TrxA-*Cv*FAP were produced in *E. coli* BL21 (DE3)-pRIL cells cultured in TB medium and purified as previously described (Sorigué et al., 2017). In brief, the first purification step for TrxA-*Cv*FAP was performed on a nickel affinity column, followed by dialysis against GF buffer (150 mM NaCl, 10 mM Tris, pH 8.0, and 5% glycerol) overnight at 4 °C. The enzyme was concentrated to approximately 40 mg·mL^{-1} using a 50-kDa Amicon Ultra centrifugal filter unit, flash-frozen in liquid nitrogen, and stored at −80 °C. For *Cv*FAP purification, the TrxA-*Cv*FAP enzyme was dialyzed in the presence of tobacco etch virus (TEV) protease (1 mg per 10 mg of total protein) after the first nickel column purification. The dialysis was performed to cleave the His-tag and TrxA, and the dialysis was performed overnight at 4 °C in a buffer containing 300 mM NaCl, 50 mM Tris (pH 8.0), 10 mM imidazole, and 5% glycerol. A second nickel affinity chromatography was performed to remove the His-tagged TrxA and TEV protease. The flow-through

Please cite this article as: Baca-Porcel Á., Samire P.P., Legeret B., Auroy-Tarrago P., Veillet F., Giacalone C., Cuine S., Moulin S., Peltier G., Li-Beisson Y., Beisson F., Sorigué D. Microbial photoproduction of *n*-heptane. Biofuel Research Journal 47 (2025) 2470-2486. DOI: 10.18331/BRJ2025.12.3.3.

containing the cleaved FAP was dialyzed into GF buffer, concentrated, flash frozen, and stored at –80 °C until use.

2.8. Measurement of fatty acid photodecarboxylase activity using membrane inlet mass spectrometry

Activity of *Cv*FAP and its N-terminal TrxA-fused variant (TrxA-*Cv*FAP) was analyzed using Membrane Inlet Mass Spectrometry (MIMS) by following the CO_2 produced during the photodecarboxylation of *n*-octanoic acid. Briefly, MIMS experiments were conducted using a Prima BT mass spectrometer (Thermo Scientific) coupled to the modified chamber of a thermo-regulated oxygen electrode chamber (Hansatech Instruments). The chamber was sealed at the bottom with a gas-permeable thin Teflon membrane (0.001-inch thickness, YSI Inc.) connected to the vacuum line of the mass spectrometer. Dissolved gases from the reaction medium diffused through the membrane into the ion source of the mass spectrometer, where $^{13}CO2$ (m/z = 45 Th) was continuously monitored (Sorigué et al., 2017; Burlacot et al., 2020). Reactions were performed in 1.5 mL of MES buffer (50 mM, pH 6.5) at 25 °C with continuous stirring. The reaction mixture contained 4 µM of FAD-containing enzyme and 1 mM of ^{13}C-labelled *n*-octanoic acid (final concentration) added as 1.5 µL of a 1 M solution in ethanol. After 1 min of incubation in the dark, the reaction was triggered by illumination using three blue LEDs (PT-54-B-L31 from Luminus; λmax 460 nm) at an intensity of 2900 µmol photons·m^{-2}·s^{-1}. $^{13}CO_2$ production was monitored for 12 min under constant light intensity.

2.9. Hydrocarbon production in 100-mL photobioreactors

To monitor the photoproduction of *n*-heptane in a 100-mL photobioreactor (turbidostat), *E. coli* cultures expressing either *Cv*FAP with *Ch*TES or *Ch*TES alone were pre-cultured in LB broth with the appropriate antibiotics. Cultures were then initiated separately at an optical density (OD600) of 0.1 in TB medium containing antibiotics, in 200-mL shake flasks with 50 mL of culture each. The cells were grown in an orbital shaker at 37 °C and 200 rpm in the dark. Once the OD600 reached ~0.8, the temperature was lowered to 20 °C and protein expression was induced using blue light at an intensity of 0.2 µmol photons·m^{-2}·s^{-1}. The cultures were grown under these conditions for 18 h.

Next, 50 mL of each *E. coli* strain culture was mixed. To prevent foaming, 0.02% antifoam 204 (v/v) was added to the TB medium. Then, 80 mL of the mixture was transferred to 100-mL photobioreactors (turbidostat) and incubated using the Multi-Cultivator MC 1000-OD from Photon Systems Instruments. Cultures were aerated with filtered air (1.5 L·min^{-1}), which proved sufficient for both growth and *n*-heptane production. A blue LED panel combined with neutral density filters (LEE® Filters) provided light intensity ranging from 75 to 300 µmol photons·m^{-2}·s^{-1}. For HC recovery, glass liners packed with activated charcoal were inserted into the air outlet of the photobioreactor and left there for 24 to 48 h to capture volatile HCs. The liners were replaced immediately after each collection period. The captured HCs were then extracted and analyzed by GC-MS/FID (see below). A schematic representation of the photobioreactor system is detailed in **Figure 6d** and **Supplementary Information, Figure S3c**. To analyze the *n*-heptane present in the liners, the activated charcoal was collected and placed in glass tubes containing 4 mL of *n*-hexane; then, the tubes were closed. The samples were shaken for 5 min and centrifuged at 3,200 g for 5 min to allow phase separation. Finally, the *n*-hexane phase was analyzed by GC-MS/FID.

2.10. Gas chromatography, coupled with mass spectrometry and flame ionization detection analyses

The mass spectrometer (MS), a GC-FID 7890B Agilent coupled to a 5977B series mass detector, was operated in full scan mode across a mass range of 40–350 Th with electron impact ionization at 70 eV. Peaks were identified based on their retention time and mass spectrum, and quantified using internal standards or external standard curves based on the FID signal (see **Supplementary Information, Fig. S3e**).

To analyze FAMEs and long-chain HCs extracted with *n*-hexane, 1 µL of the *n*-hexane phase was injected (splitless injection at 250 °C) onto an HP-5MS column (length: 30 m; inner diameter: 0.250 mm; film thickness: 0.25 µm). Helium (1.4 mL·min^{-1}) was the carrier gas, and liquid nitrogen was used to decrease the oven temperature. The oven temperature program was as follows: initial temperature of 50 °C for 1 min, ramping at 20 °C·min^{-1} to 160 °C, then at 10 °C·min^{-1} to 300 °C, and maintaining the final temperature for 1 min. The same parameters were used to analyze *n*-heptane extracted in *n*-hexane, except that the initial oven temperature was set to 5 °C using liquid nitrogen to cool the column.

To analyze volatile HCs by headspace, one mL of the gas phase (headspace) from the sealed vials was collected with a preheated syringe (80 °C) and injected (split injection ratio 1:10) onto an HP-PLOT Q column (length 30 m, inner diameter 0.32 mm, film thickness 20 µm). Helium was the carrier gas at a flow rate of 1.4 mL·min^{-1}. The oven temperature program was as follows: initial temperature of 50 °C for one min; ramp of 20 °C·min^{-1} to 260 °C, maintained for 20 min.

Quantification of *n*-heptane was carried out using a standard calibration curve prepared by adding different concentrations of *n*-heptane to *E. coli* cells carrying a pDawn empty vector at an OD600 of 7 to mimic the experimental matrix. For purity analysis, peaks were identified based on their retention times and mass spectra. Quantification was performed using the FID signal, and the purity of *n*-heptane was estimated by calculating the ratio of the *n*-heptane peak area to the total integrated FID signal of all detected peaks in the sample.

3. Results and Discussion

3.1. Effect of Thioredoxin-A fusion on the fatty acid photodecarboxylase activity in Escherichia coli

In our previous studies on FAP, the recombinant protein was systematically fused to *E. coli* TrxA in the N-terminus because it was initially observed that the TrxA-FAP fusion shows increased solubility during the FAP purification process (Sorigué et al., 2017). However, the benefit of TrxA presence for the activity of FAP in *E. coli* cells was not evaluated. Therefore, to determine whether the metabolic burden created by the addition of TrxA was necessary for hydrocarbon synthesis in *E. coli*, the most characterized and widely used FAP homolog, *Cv*FAP, was expressed in *E. coli* BL21(DE3) cells, either fused to TrxA or not, under the control of the IPTG-inducible promoter system (T7). The results clearly show that *Cv*FAP fused with TrxA resulted in a 12-fold and an 8-fold increase in total HC content at 24 h, and 48 h post-induction respectively (**Fig. 1a**) while cell concentrations were similar with and without TrxA (**Fig. 1b**). Although TrxA fusion slightly changed the HC profile, the species produced remained mainly C15-C17 alka(e)nes (**Fig. 1c**). Protein and immunoblot analysis of total and soluble fractions indicated that the expression level of *Cv*FAP fused with TrxA was much higher after 24 and 48 h of induction with IPTG compared to *Cv*FAP alone (**Fig. 1d** and **Supplementary Information, Fig. S1a–d**). This observation suggested that TrxA also helped with the solubility and/or stability of FAP *in vivo*.

It was also observed that TrxA-*Cv*FAP, but not TrxA alone, increased the total fatty acid content with a more significant effect at 48h (**Supplementary Information, Fig. S2a**). The presence of *Cv*FAP also drastically changed the fatty acid profile by increasing the amount of cis-9-octadecenoic acid (C18:1 fatty acid) and decreasing methyleneoctadecanoic and methylenehexadecanoic acids significantly compared to control strains (**Supplementary Information, Fig. S2c**). These changes suggest a metabolic adaptation of the host to compensate for fatty acid depletion and/or accumulation of HCs caused primarily by *Cv*FAP.

The beneficial effect of TrxA fusion is likely due to the increased level of total *Cv*FAP expressed in *E. coli* (**Fig. 1d**). However, this effect could also result from a more complex mechanism, in which TrxA fusion enhances catalytic efficiency by increasing enzyme solubility or facilitating substrate accessibility. To investigate these possibilities, *Cv*FAP and TrxA-*Cv*FAP proteins were purified and characterized *in vitro*. MIMS was used to measure CO_2 production resulting from the photodecarboxylation of *n*-octanoic acid (**Fig. 1e**). The absence of a significant difference between *Cv*FAP and TrxA-*Cv*FAP indicates that the increased activity observed *in vivo* is essentially due to higher *Cv*FAP expression rather than an intrinsic

Please cite this article as: Baca-Porcel Á., Samire P.P., Legeret B., Auroy-Tarrago P., Veillet F., Giacalone C., Cuine S., Moulin S., Peltier G., Li-Beisson Y., Beisson F., Sorigué D. Microbial photoproduction of *n*-heptane. Biofuel Research Journal 47 (2025) 2470-2486. DOI: 10.18331/BRJ2025.12.3.3.

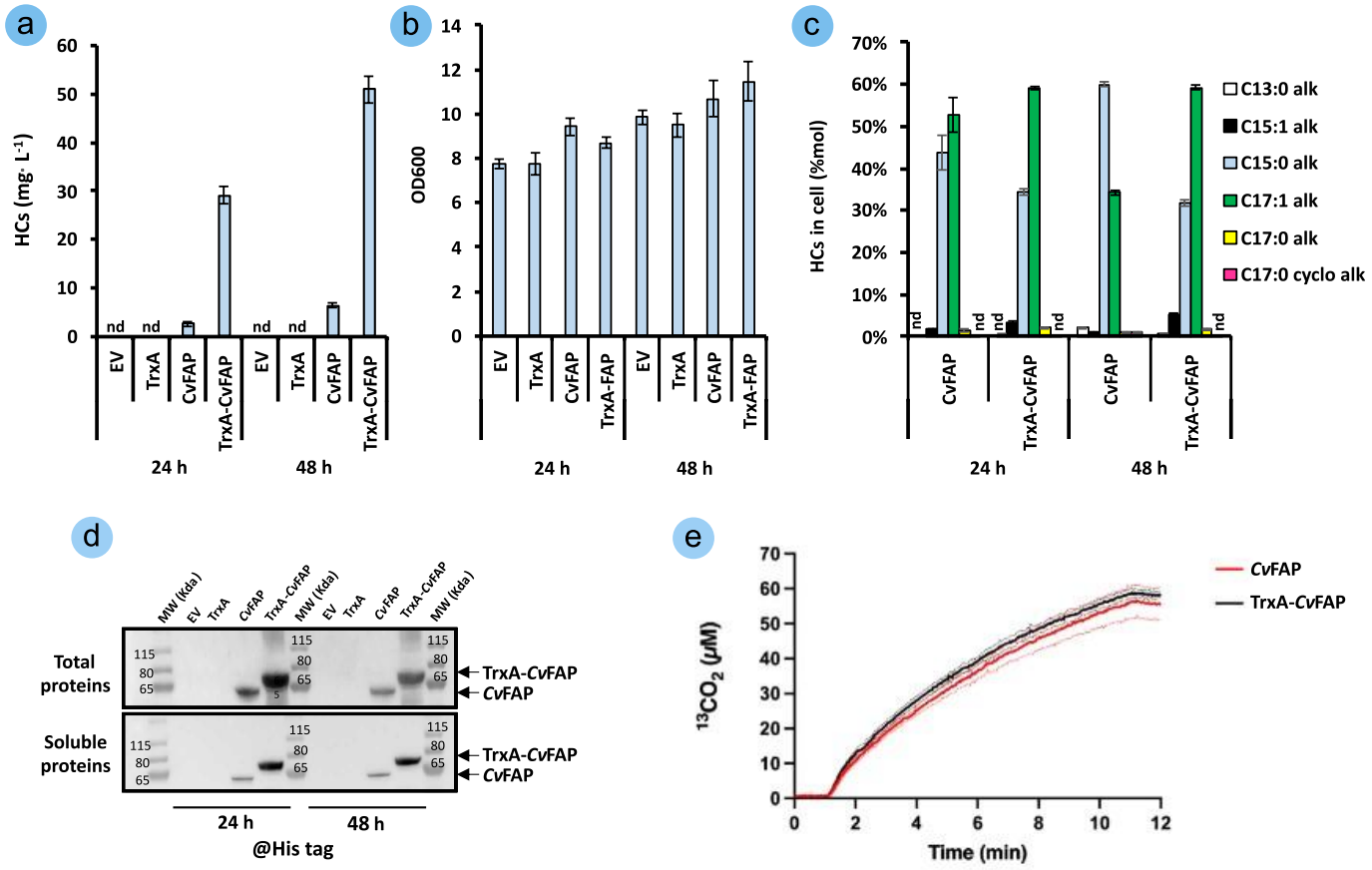

Fig. 1. Effect of TrxA fusion on *Cv*FAP expression and HC production in *E. coli*. a) HCs levels in *E. coli* cells expressing *Cv*FAP ± TrxA fusion after 24- or 48-h of induction with 0.5mM IPTG under blue light (100 µmol photons·m^{-2}·s^{-1}). **b)** Optical density of corresponding cultures. **c)** HCs profiles in cells expressing *Cv*FAP ± TrxA fusion. Error bars represent the standard error (n=3). 'nd' = not detected. C17 cyclo alk = methyleneheptadecane. **d)** Immunoblot of *Cv*FAP in total and soluble fractions normalized based on cell concentration at 24 and 48 h post-induction. **e)** Photocatalytic activity of *Cv*FAP and TrxA-*Cv*FAP (normalized on FAD content) measured by monitoring $^{13}CO_2$ release during the decarboxylation of *n*-hexadecanoic acid-1-^{13}C using MIMS. The standard error for FAP and TrxA-*Cv*FAP is shown as red and black dashed lines, respectively.

change in enzymatic activity due to the fusion. The overall positive effect on the total HC production clearly shows that TrxA fusion should be used in any biocatalytic or bioconversion process involving *Cv*FAP. The substantial enhancement in *Cv*FAP expression and HC production due to TrxA fusion led us to systematically employ TrxA-FAP fusions in all subsequent experiments.

3.2. Test of fatty acid photodecarboxylase homologs for n-heptane production

To date, *Cv*FAP is the only documented producer of *n*-heptane (Yunus et al., 2022; Samire et al., 2023). In exploring the conservation of FAP activity in various microalgae, a few other homologs (**Table 2**) with demonstrated photodecarboxylase activity were previously identified (Moulin et al., 2021; Zeng et al., 2022; Ma et al., 2023). These studies suggested that some of these homologs may have different substrate specificity profiles than *Cv*FAP; however, activity on *n*-octanoic acid was not tested. Therefore, the capacity of five selected FAPs for *n*-heptane production was assessed. To simplify the screening process, *n*-octanoic acid was added directly to the culture medium. The effect of *n*-octanoic acid on cell viability was first evaluated by adding various concentrations of this compound to *E. coli* cells containing an empty vector. Concentrations below 4 mM did not affect cell viability (**Fig. 2a**). Therefore, a concentration of 2 mM was selected for further experiments. The first set of experiments showed that in an empty vector strain grown in the dark for 16 h, *n*-octanoic acid could be detected inside the cells as early as 2 h after its addition to the medium (**Fig. 2b**). FAP homologs were expressed under the control of the IPTG-inducible T7. The growth of *E. coli* strains was slightly affected by the expression of FAPs except for *Gs*FAP (**Fig. 2c**). SDS-PAGE and immunoblot analyses indicated that all FAPs were well expressed. Only *Cv*FAP, *Cr*FAP, *Cc*FAP, and *Ng*FAP were detected in the soluble fraction, with *Cv*FAP being the most abundant (**Fig. 2d** and **Supplementary Information, Fig. S1e-h**). To measure the *n*-heptane production capacity of each strain expressing an FAP, the shake flask cultures pre-incubated with *n*-octanoic acid were exposed to 300 µmol photons·m^{-2}·s^{-1} of blue light for 20 min in sealed vials, after which *n*-heptane was measured in the gas phase. All of the tested FAP homologs were active on *n*-octanoic acid; however, the *n*-heptane levels varied considerably, and the highest *n*-heptane production was obtained with *Cv*FAP (**Fig. 2e**). *Cv*FAP (fused to TrxA) outperforms other FAP homologs (also fused to TrxA) in *n*-heptane production *in vivo*. This could be due in part to lower amounts of soluble FAP form (**Fig. 2d** and **Supplementary information, Fig. S1e-h**). However, differences in FAPs stability and turnover on *n*-octanoic acid cannot be ruled out. In practice, the strain harboring *Cv*FAP demonstrated the greatest capacity to convert *n*-octanoic acid to *n*-heptane, so it was selected for subsequent studies.

3.3. Comparison of IPTG and blue light-inducible promoters for n-heptane production

To streamline a bioprocess and eliminate the need for chemical inducers, a light-inducible promoter was investigated for controlling *Cv*FAP

Please cite this article as: Baca-Porcel Á., Samire P.P., Legeret B., Auroy-Tarrago P., Veillet F., Giacalone C., Cuine S., Moulin S., Peltier G., Li-Beisson Y., Beisson F., Sorigué D. Microbial photoproduction of *n*-heptane. Biofuel Research Journal 47 (2025) 2470-2486. DOI: 10.18331/BRJ2025.12.3.3.

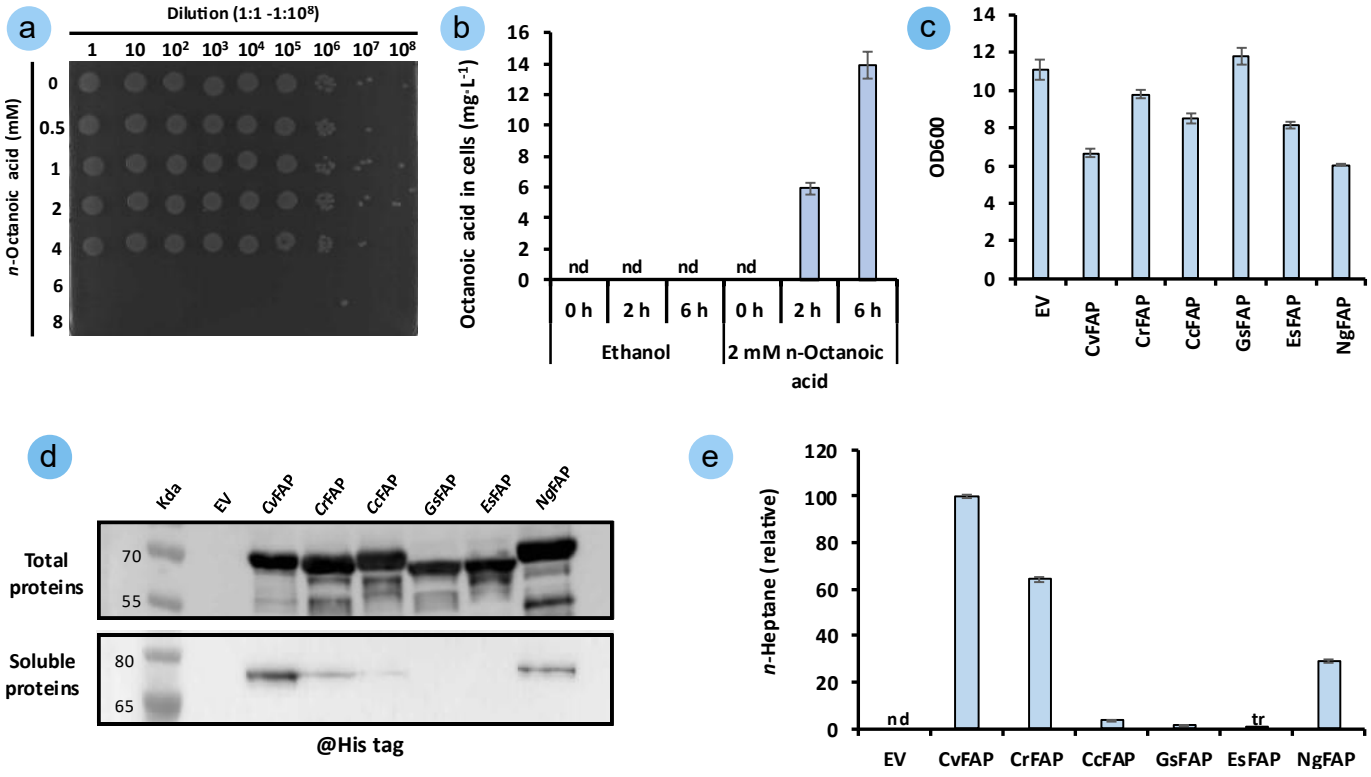

Fig. 2. *n*-Heptane production by *E. coli* expressing various FAPs homologs. a) Drop test assessing the viability of *E. coli* cells harboring an empty vector (EV) exposed to increasing *n*-octanoic acid concentrations. **b)** Time course of *n*-octanoic acid uptake by *E. coli* (EV) control cells treated with 2 mM *n*-octanoic acid (in ethanol). Strains exposed only to ethanol served as controls. **c)** Optical density of strains expressing FAP homologs after a 16-h cultivation period. **d)** Immunoblot of FAP homologs in total and soluble after a 16-h culture period in the dark, normalized based on cell concentration. **e)** Comparative *n*-heptane production by *E. coli* strains expressing different FAP homologs compared to EV. Cultures were grown in the dark for 16 h, supplemented with 2 mM *n*-octanoic acid for 2 h, then illuminated under 300 µmol photons·m^{-2}·s^{-1} of blue light in sealed vials for 20 min at 20 °C. Error bars represent the standard error (n=3). 'nd' = not detected, 'tr'= traces.

expression. The blue light-inducible plasmid pDawn (Ohlendorf et al., 2012) was selected, as blue light also triggers FAP enzymatic activity. In other words, the blue light used to illuminate cells can also facilitate the constant replacement of FAP, which is prone to photoinactivation (Lakavath et al., 2020). Therefore, to control the expression of *Cv*FAP, the gene was expressed in *E. coli* using a plasmid under the control of either the blue light-inducible promoter or the IPTG-inducible T7 promoter. The different *E. coli* strains were then exposed to 2 mM *n*-octanoic acid, and *n*-heptane production was compared between the two expression systems.

First, the performances of pDawn and the IPTG-inducible promoter T7 were compared by inducing expression with varying light intensities (0 to 1.2 µmol photons·m^{-2}·s^{-1}) and IPTG concentrations (0–2 mM), respectively. Cell growth was decreased with increasing IPTG concentrations and remained constant with increasing light intensities (**Fig. 3a**). Interestingly, when *n*-heptane production was compared in an *E. coli* strain expressing *Cv*FAP under the control of either pDawn or T7, only a 20% increase was observed with IPTG induction compared to light (**Fig. 3b**). These results demonstrate that the T7 promoter can be effectively replaced with the blue light-inducible promoter for the expression of *Cv*FAP. Using pDawn, a light intensity of 0.2 µmol photon·m^{-2}·s^{-1} was found to yield the highest level of *n*-heptane production, and this condition was selected for induction. Owing to the low light requirement, only minimal energy is needed to provide sufficient blue light for pDawn activation, which may help prevent FAP photoinactivation during the induction phase. The effect of *n*-octanoic acid on *E. coli* cells expressing *Cv*FAP under pDawn control was also evaluated.

3.4. Selection of an octanoyl-ACP-specific thioesterase for endogenous substrate supply

Several *n*-octanoic acid-producing thioesterases (C8TESs) from plants and bacteria were evaluated to construct an *E. coli* strain expressing FAP and capable of synthesizing *n*-octanoic acid (Dehesh et al., 1996; Jing et al., 2011). These included an improved variant from *Cuphea palustris* (Hernández Lozada et al., 2018) (**Table 2**). C8TESs interrupt the fatty acid elongation pathway by hydrolyzing octanoyl-ACP intermediates specifically, thereby releasing *n*-octanoic acid within the cell (**Fig. 4a**). The thioesterase sequences were codon-optimized for *E. coli* expression. The co-expression of the C8TES and *Cv*FAP genes was performed in an operon under the control of the blue light-inducible promoter. Protein expression was induced with 0.2 µmol photons·m^{-2}·s^{-1} of blue light. Growth of *E. coli* strains was only slightly affected by co-expressing *Cv*FAP and different C8TESs compared to expressing *Cv*FAP alone (**Fig. 4b**). As expected, co-expressing each thioesterase with *Cv*FAP resulted in *n*-octanoic acid formation (**Fig. 4c**). The thioesterase from *Cuphea hookeriana* (*Ch*TES) produced the most acid, even at a low expression level (see **Supplementary Information, Fig. S1i-j**).

The cultures were then exposed to 300 µmol photons·m^{-2}·s^{-1} in sealed vials for 4 h to trigger HC production. The expression of C8TESs drastically increased the total HC content in the vial's gas phase, with the highest amount obtained with *Ch*TES (**Fig. 4d**). Kinetics of *n*-heptane production, performed on the *Ch*TES + *Cv*FAP strain, indicated that *n*-heptane synthesis stopped after 2 h of illumination, reaching a titer of around 12.5 mg·L^{-1} of culture (**Fig. 4e**). The composition of the HCs collected in the gas phase was similar for the three C8TESs, with over 90% *n*-heptane and the remainder *n*-nonane and *n*-nonene (**Fig. 4f**). Assessing the distribution of *n*-heptane between the gas phase and cells in the *Ch*TES + *Cv*FAP strain revealed that nearly 90% was in the gas phase (**Fig. 4g**). Inside the cells, in addition to residual *n*-heptane, longer HCs were detected, primarily *n*-pentadecane and *n*-heptadecene (**Fig. 4h–i**).

In an attempt to further increase *n*-heptane production, the *Ch*TES + *Cv*FAP construct was tested in various *E. coli* expression strains. However,

Please cite this article as: Baca-Porcel Á., Samire P.P., Legeret B., Auroy-Tarrago P., Veillet F., Giacalone C., Cuine S., Moulin S., Peltier G., Li-Beisson Y., Beisson F., Sorigué D. Microbial photoproduction of *n*-heptane. Biofuel Research Journal 47 (2025) 2470-2486. DOI: 10.18331/BRJ2025.12.3.3.

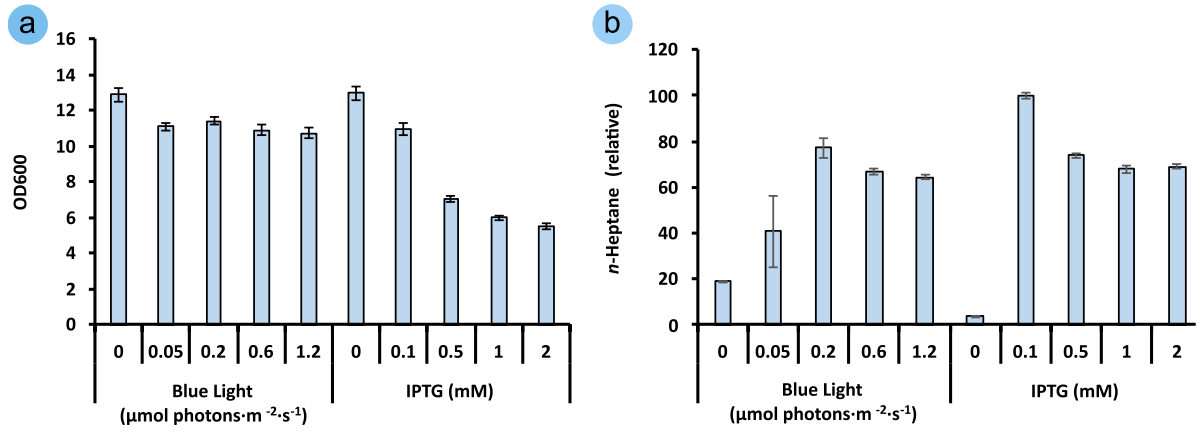

Fig. 3. Effect of inducible promoters on *n*-heptane production using *Cv*FAP. a) Cell growth and **b)** *n*-Heptane production of *E. coli* expressing *Cv*FAP under the light-inducible or IPTG-inducible promoter promoters. Enzyme expression was induced with different light intensities or IPTG concentrations. For HC quantification, cultures were incubated with 2 mM *n*-octanoic acid for 2 h in the dark, followed by 20 min of blue light (300 µmol photons·m^{-2}·s^{-1}). Error bars represent the standard error (n=3) for growth measurement and (n=5) for HC quantifications.

all six alternative strains showed equal or lower heptane production compared to the BL21(DE3) pRIL strain (**Fig. 5a**).

From these initial experiments, it was evident that strains with different C8TESs exhibited varying capacities for producing *n*-heptane. In anticipation of future optimization, it was crucial to ascertain whether factors other than thioesterase activity could influence this capacity. Cell concentration after induction was only slightly higher in the three C8TES strains (**Fig. 4b**). Additionally, the C8TESs had no significant effect on the total amount of fatty acids, except for the *At*TES + *Cv*FAP strain, which exhibited a decrease in total fatty acids (see **Supplementary Information, Fig. S2b**). This outcome contrasts with the enhancement in fatty acid synthesis observed with the expression of a plant C12-specific TES in *E. coli* (Moulin et al., 2019). Regarding the *n*-heptane precursor, *n*-octanoic acid represented 5–7.4% of total fatty acids before illumination and 3.5–11% after illumination in the three strains (see **Supplementary Information, Fig. S2d-e**). Interestingly, *Ch*TES was the most effective in producing *n*-octanoic acid both before and after illumination and was the only C8TES for which the content of *n*-octanoic acid was higher after illumination than before (**Fig. 4c**). Another factor that may explain the differences in *n*-heptane production is the unequal level of *Cv*FAP expression in the three strains (see **Supplementary Information, Figs. S1i** and **S1j**). The results indicated that the level of *n*-heptane was likely the result of a complex interplay between *Cv*FAP and C8TES expression.

To test if *n*-octanoic acid levels limit *n*-heptane formation in the best strain obtained thus far (*Ch*TES + *Cv*FAP), post-induction cells were incubated in the dark for 2 h with various *n*-octanoic acid concentrations (0–6 mM) before being illuminated at 300 µmol photons·m^{-2}·s^{-1}. While the addition of exogenous *n*-octanoic acid did not significantly impact cell viability (**Fig. 5b**), a notable increase in *n*-heptane production was evident (**Fig. 5c**). These results suggest that *n*-octanoic acid was indeed a limiting factor in the *Ch*TES + *Cv*FAP strain. However, such an interpretation appears contradictory to the observed accumulation of *n*-octanoic acid over time in this strain (**Fig. 4c**). The apparent discrepancy can be explained by considering the dynamics of fatty acid production and FAP photoinhibition (Moulin et al., 2019; Lakavath et al., 2020). Adding a large quantity of exogenous *n*-octanoic acid may protect FAP from photoinhibition by preventing FAD triplet formation, thereby leading to higher alkane production, as has been proposed for in vitro FAP activity (Samire et al., 2023). Although FAP is supposed to renew itself through promoter induction continually, its synthesis may not completely compensate for photodegradation. Over time, as FAP degrades due to photoinhibition, *n*-octanoic acid production persists through *Ch*TES, which may explain its accumulation. Identifying FAP mutants that are less prone to photoinhibition is an important goal for further increasing HC production.

3.5. Improvement of the n-heptane production by the E. coli strain expressing ChTES and CvFAP.

Previous observations have shown that the availability of *n*-octanoic acid limits *n*-heptane production by the *Ch*TES + *Cv*FAP strain (**Fig. 5c**). One possible explanation is that *E. coli* strains that express different C8TESs secrete significant amounts of fatty acids into the culture medium, as has been shown for various thioesterases (Jing et al., 2011). To test this hypothesis, the amount of *n*-octanoic acid was measured in both the supernatant and the cells of *E. coli* strains expressing different C8TESs using the pDawn blue light-inducible system, after 18 h of cultivation under 0.2 µmol photons·m^{-2}·s^{-1} of blue light. Compared to the empty vector (EV), growth was positively impacted by *Ch*TES or *At*TES but negatively affected by CpTES-287 (see **Supplementary Information, Fig. S3a**). For all three thioesterases, most of the *n*-octanoic acid was found in the supernatant, while only a small amount remained intracellularly (**Fig. 6a**). Among the different strains, *Ch*TES produced the highest yield of *n*-octanoic acid (344.4 mg·L^{-1}). Based on these results, various strategies were tested to enhance *n*-heptane production by supplementing the *Ch*TES + *Cv*FAP strain with *n*-octanoic acid produced by the *Ch*TES-expressing strain. The *Ch*TES strain secretes *n*-octanoic acid into the supernatant; therefore, the *Ch*TES + *Cv*FAP strain utilizes both endogenous and exogenous *n*-octanoic acid to produce *n*-heptane (**Fig. 6b**).

To optimize the supply of *n*-octanoic acid produced by bacterial cells to the photodecarboxylase, a strategy was explored in which a strain co-expressing *Cv*FAP and *Ch*TES was co-cultivated with an *E coli* strain expressing only *Ch*TES. Four variations of this strategy were evaluated: the two strains are first cultivated separately and then mixed in different ratios (conditions 1 to 3), or the two strains were cultivated together since the initial pre-culture (condition 4). These four conditions were compared to the cultivation of the strain co-expressing *Cv*FAP and *Ch*TES (in the presence or absence of exogenous fatty acids). The optical density of the different cell cultures was measured, and the growth of the strain co-expressing *Ch*TES and *Cv*FAP was found to be slightly higher (**Supplementary Information, Fig. S3b**). Strikingly, regarding *n*-heptane production after 4 h of illumination upon mixing of the strains (**Fig. 6c**), all cultures mixing two strains outperformed the culture with the co-expression by at least 11-fold, corresponding to 50 to 70% of the value obtained with an exogenous supply of 2 mM fatty acids to the co-expression. Co-cultivation of a strain expressing both enzymes and a strain specialized in producing fatty acids was therefore highly efficient in increasing *n*-heptane production. Even if there were some slight differences between the four tested conditions, condition 3 was selected for upscaling due to its simplicity, as it involved mixing equal volumes of each culture.

Please cite this article as: Baca-Porcel Á., Samire P.P., Legeret B., Auroy-Tarrago P., Veillet F., Giacalone C., Cuine S., Moulin S., Peltier G., Li-Beisson Y., Beisson F., Sorigué D. Microbial photoproduction of *n*-heptane. Biofuel Research Journal 47 (2025) 2470-2486. DOI: 10.18331/BRJ2025.12.3.3.

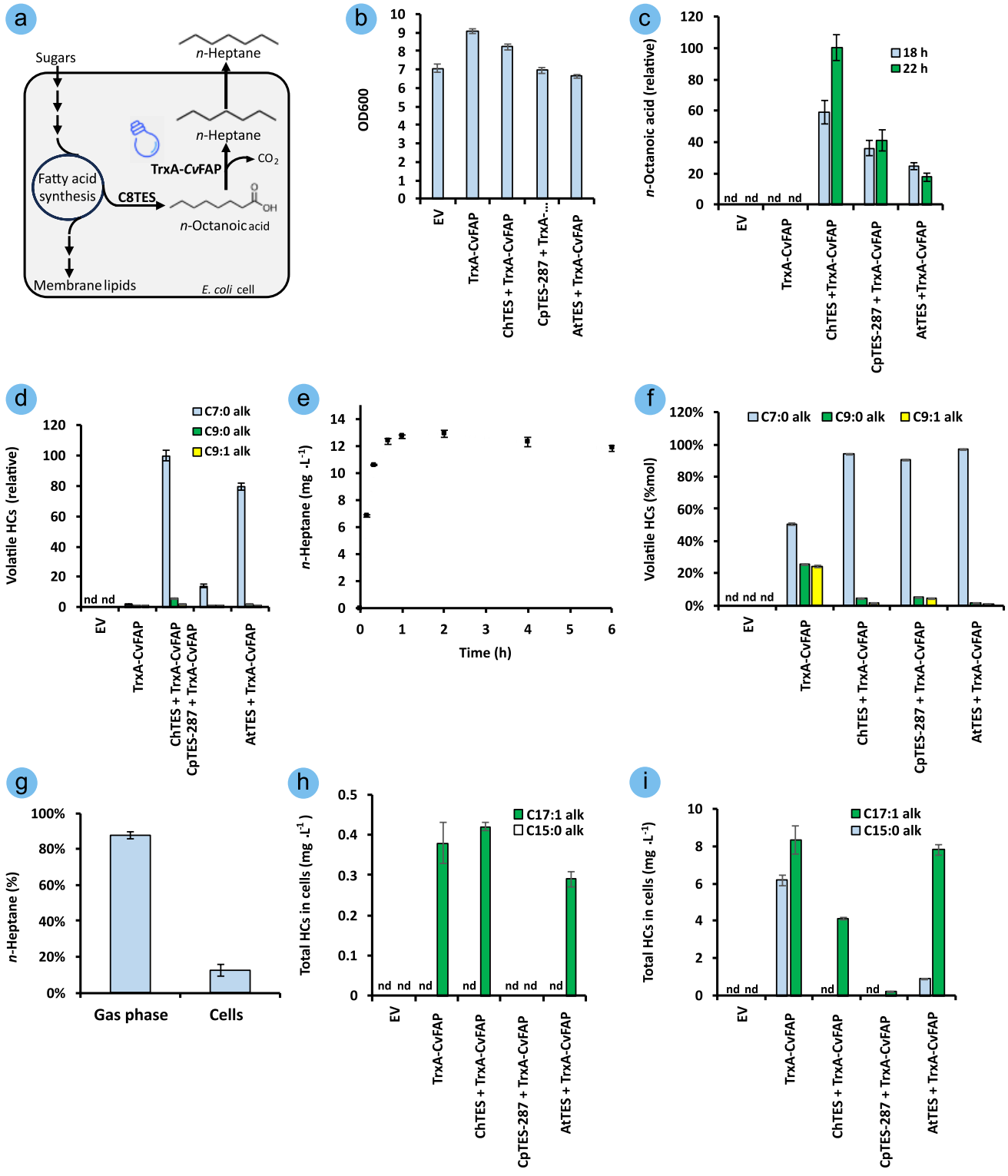

Fig. 4. HC production in *E. coli* cells co-expressing *Cv*FAP and various C8-specific thioesterases. a) Schematic representation of the engineered *n*-heptane biosynthetic pathway using C8TESs and *Cv*FAP. **b)** Optical density of the different strains after 18 h of culture under 0.2 µmol photons·m^{-2}·s^{-1} of blue light. **c)** *n*-Octanoic acid content of the different strains before (18 h) and 4 h after (22 h) illumination at 300 µmol photons·m^{-2}·s^{-1} of blue light. **d)** Volatile HCs in the headspace of the different strains after 4 h of blue light (300 µmol photons·m^{-2}·s^{-1}). **e)** Kinetics of *n*-heptane release in the headspace of the *Ch*TES + *Cv*FAP strain under 300 µmol photons·m^{-2}·s^{-1} of blue light. **f)** HCs profile in headspace after 4 h of light in strains co-expressing different C8TESs with *Cv*FAP. **g)** Distribution of *n*-heptane between headspace and culture medium of *Ch*TES + *Cv*FAP strain. **h)** & **i)** Intracellular long-chain-HC content **(h)** before and **(i)** after a 4 h of blue light (300 µmol photons·m^{-2}·s^{-1}). An empty vector strain was used as a control. Error bars represent the standard error (n=3). 'nd' = not detected.

Please cite this article as: Baca-Porcel Á., Samire P.P., Legeret B., Auroy-Tarrago P., Veillet F., Giacalone C., Cuine S., Moulin S., Peltier G., Li-Beisson Y., Beisson F., Sorigué D. Microbial photoproduction of *n*-heptane. Biofuel Research Journal 47 (2025) 2470-2486. DOI: 10.18331/BRJ2025.12.3.3.

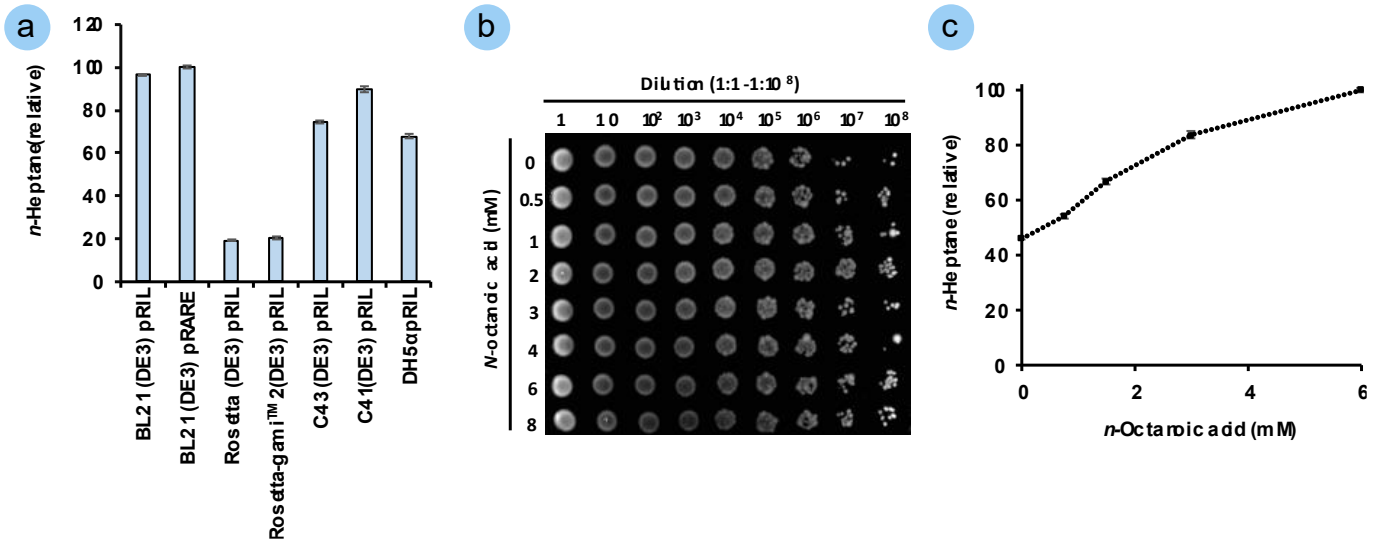

Fig. 5. Hydrocarbon production by *E. coli* BL21(DE3) co-expressing *Cv*FAP and *Ch*TES under pDawn. a) Relative *n*-heptane production in different *E. coli* strains after 4 h of blue light (300 µmol photons·m^{-2}·s^{-1}). **b)** Drop test assessing the viability of *E. coli* cells expressing *Ch*TES + *Cv*FAP exposed to increasing *n*-octanoic acid concentrations. After protein induction (16 h with 0.2 µmol photons· m^{-2}·s^{-1} of blue light), cultures were treated with different concentrations of *n*-octanoic acid for 2 h just before the drop test. **c)** Total *n*-heptane level in the *Ch*TES + *Cv*FAP strain fed with increasing concentrations of *n*-octanoic acid and exposed to blue light (300 µmol photons·m^{-2}·s^{-1}) for 4 h at 20 °C. Error bars represent the standard error (n=3). 'nd' = not detected.

3.6. Photoproduction of n-heptane in 100 mL photobioreactors

To evaluate *n*-heptane production on a larger scale, a 100-mL photobioreactor was used (see **Fig. 6d** and **Supplementary Information, Fig. S3c**). Both strains were cultured separately for 18 h under 0.2 µmol photons·m^{-2}·s^{-1} of blue light and exhibited similar growth (see **Supplementary Information, Fig. S3d**). Then, the cultures were mixed at a 1:1 ratio and transferred into the photobioreactors. The combined cultures were then incubated for 128 h at 20 °C with an airflow rate of 1.5 L·min under different light intensities to evaluate their effect on *n*-heptane production. The highest *n*-heptane production was observed at 75 µmol photons·m^{-2}·s^{-1} of blue light, yielding a cumulative *n*-heptane concentration of 286 mg·L^{-1} with an average productivity of 2.23 mg·L^{-1}·h^{-1} (53.5 mg·L^{-1}·d^{-1}) after 128 h of culture (**Fig. 6e**).

The majority of *n*-heptane synthesis occurred within the first 56 h, during which approximately 272 mg·L^{-1} was produced, corresponding to a productivity of 4.9 mg·L^{-1}·h^{-1}. After this period, *n*-heptane production plateaued, possibly due to nutrient depletion, pH reduction, enzyme degradation, or FAP photoinhibition. Previous studies have reported lower *n*-heptane yields. For example, an engineered *Synechocystis* sp. PCC 6803 that expresses *Cv*FAP and C8TES from *Cuphea palustris*, among other modifications, produced approximately 5 mg·L^{-1} of culture over 10 d (0.48 mg·L^{-1}·d^{-1}) (Yunus et al., 2022). Additionally, in the production of longer-chain HCs, an engineered *E. coli* strain produced 328 mg·L^{-1} of *n*-nonane and other longer-chain HCs, including *n*-dodecane, *n*-tridecane, 2-methyl-dodecane, and *n*-tetradecane, though the cultivation time was not specified, precluding a productivity comparison (Choi and Lee, 2013). Thus, our results demonstrate a significant improvement in *n*-heptane production through a co-cultivation strategy compared to similar studies (**Table 1**).

4. Conclusions and future perspectives

This work developed a microbial platform for *n*-heptane photoproduction. *Cv*FAP was fused to TrxA, which increased its biological activity. Various FAP homologs were tested, and *Cv*FAP was identified as the most effective enzyme for in vivo *n*-heptane synthesis. To produce *n*-octanoic acid *in situ*, *Cv*FAP was co-expressed with various thioesterases. The thioesterase from *Cuphea hookeriana* was identified as the most effective for *n*-heptane production. Using a strategy in which the strain expressing FAP was co-cultivated in photobioreactors with a strain specialized in fatty acid production, scale-up to a 100 mL photobioreactor yielded a cumulative titer of 272 mg·L^{-1} over 56 h, corresponding to an average productivity of 4.9 mg·L^{-1}·h^{-1} (117 mg·L^{-1}·d^{-1}). Such performance represented a significant increase in productivity compared to previous studies (**Table 1**) and may be partly due to the recovery of HC in the gas phase. As previously observed for *n*-undecane (Moulin et al. 2019) and reported here for *n*-heptane, long-chain HCs accumulate within the cells, while shorter chains tend to diffuse out. The intracellular accumulation of HC can be both limiting and toxic to the cells. Therefore, the facilitated diffusion of shorter alkanes to the culture medium and subsequently into the gas phase may alleviate this toxicity. Splitting the pathway across two microbial platforms was also found to be an effective method for boosting titers, as the division allows each metabolic pathway to be optimized and may reduce the overall metabolic burden. Using this strategy, the HC titer was increased 11-fold.

This work provides a fundamental framework for the microbial synthesis of medium-chain HCs and will hopefully contribute to more sustainable fuel production that is less dependent on fossil resources. However, the current titers remain below the threshold for industrial fuel processing. Several options remain to be explored in future studies.

Continuous blue light was used throughout experiments, which may lead to *Cv*FAP photoinactivation. Several strategies can be used to overcome this limitation, either based on light management or enzyme optimization. Recent studies (Spacey et al., 2025) show that switching to pulsed violet illumination can drastically increase activity. Using pulsed blue LEDs or UV flashes in the reactor could also increase productivity. Regarding enzyme robustness, radical-based photoinactivation remains a significant challenge. One interesting strategy is the continuous cultivation of the strains to renew biocatalyst pools and directed evolution to reduce the flavin's side reactions.

Concerning photobioreactor geometry and scaling up, flat-panel photobioreactors have a better surface-to-volume ratio than tubular systems (Chanquia et al., 2021). Switching from rich to low-cost mineral media and integrating the FAP and thioesterase pathways chromosomally to remove antibiotic selection and reduce genetic drift could also reduce costs in terms of process integration and medium cost. Improving the metabolic flux balance could also impact alkane production. As previously demonstrated by some authors, fine-tuning of engineered *E. coli* strains led to an increase in titer from 2.8 mg·L^{-1} to 425 mg·L^{-1} in shake flasks (approximately 148-fold increase) and subsequently to 2.54 g·L^{-1} in a 5-L fed-batch run (Fatma

Please cite this article as: Baca-Porcel Á., Samire P.P., Legeret B., Auroy-Tarrago P., Veillet F., Giacalone C., Cuine S., Moulin S., Peltier G., Li-Beisson Y., Beisson F., Sorigué D. Microbial photoproduction of *n*-heptane. Biofuel Research Journal 47 (2025) 2470-2486. DOI: 10.18331/BRJ2025.12.3.3.

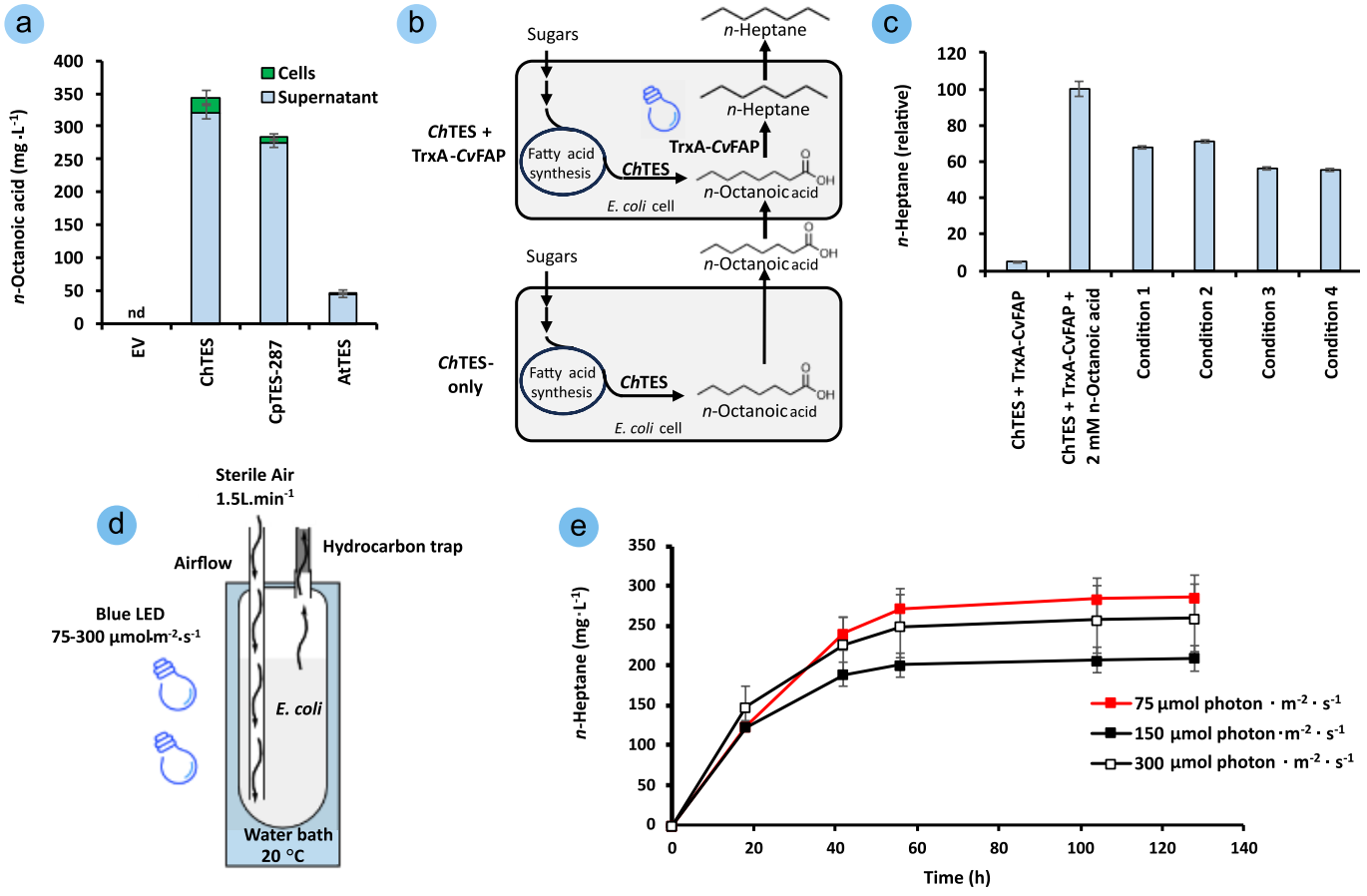

Fig. 6. Optimizing *n*-Heptane photoproduction using co-culture and test in a 100-mL photobioreactor. a) Intra- and extracellular *n*-octanoic acid content in *E. coli* expressing different C8TESs after 18 h of induction at 0.2 µmol photons·m^{-2}·s^{-1} of blue light. **b)** Schematic representation of the combination of *E. coli* strains co-expressing *Ch*TES + *Cv*FAP with *Ch*TES-only strains to increase *n*-octanoic supply. **c)** *n*-Heptane production under various mixing conditions (1–4) of *Ch*TES + *Cv*FAP and *Ch*TES strains. Condition 1: Pelleted cells from *Ch*TES + *Cv*FAP combined with an equal volume of *Ch*TES culture. Condition 2: Pelleted cells from *Ch*TES + *Cv*FAP cultured combined with half the volume of the *Ch*TES culture. Condition 3: Mix of *Ch*TES + *Cv*FAP culture and *Ch*TES culture at a 1:1 (v/v) ratio. Condition 4: Co-culture of *Ch*TES + *Cv*FAP and *Ch*TES strain. Controls: strain co-expressing *Cv*FAP and *Ch*TES ± *n*-octanoic acid (2 mM). **d)** Schematic of the 100 mL photobioreactor system equipped with adjustable light, temperature, airflow, and volatile HC capture system. **e)** Cumulative *n*-heptane production over 128 h in a 100-mL photobioreactor by a co-culture (1:1 v/v) of the *Ch*TES and *Ch*TES + *Cv*FAP strains. The co-culture was grown in batch under continuous blue light (75–300 µmol photons·m^{-2}·s^{-1}) and 1.5 L·min^{-1} airflow at 20 °C. Error bars represent the standard error (n=3). 'nd' = not detected.

et al. 2018). A similar strategy could be employed to increase the production of *n*-octanoic acid and *n*-heptane. Addressing interconnected factors such as light, enzyme stability, reactor geometry, and metabolic optimization of fatty acid flux could further improve the competitiveness of the described co-cultivation strategy for enzymatic photoproduction. This work establishes a fundamental framework for the microbial synthesis of medium-chain HCs, which could contribute to more sustainable fuel production and reduce dependence on fossil resources.

Acknowledgements

We would like to thank Dr. Laurence Blanchard for helpful discussions, and Dr. Pei Ge and Louise Ardouin for technical help. This work was funded in part by the French National Research Agency project Photoalkane (ANR-18-CE43-0008). The funding provided by the European Regional Development Fund (ERDF), the Région Provence Alpes Côte d'Azur, the French Ministry of Research, and the CEA for the HélioBiotec platform is also acknowledged. A.B.P. was supported by a PhD fellowship "Economie Circulaire du Carbone" from CEA. D.S.'s work was supported by CEA and by a Marie Sklodowska-Curie Actions global fellowship (Project 101063280 - EXPERIMENTAL).

Author contributions

Ángel Baca-Porcel: Conceptualization, Methodology, Investigation, Formal analysis, Data curation, Visualization, Writing - original draft, review & editing. **Poutoum Palakiyém Samire:** Methodology, Investigation, Formal analysis, Data curation, Discussion. **Bertrand Légeret:** Methodology, Validation, Investigation, Formal analysis, Data curation, Supervision, Discussion. **Pascaline Auroy-Tarrago:** Methodology, Supervision. **Florian Veillet:** Supervision, Methodology, Investigation, Formal analysis, Discussion. **Cécile Giacalone:** Investigation, Formal analysis. **Stéphan Cuine:** Methodology, Investigation, Formal analysis. **Solène Moulin:** Investigation, Formal analysis, Discussion. **Gilles Peltier:** Methodology, Investigation, Formal analysis, Data curation, Discussion. **Yonghua Li-Beisson:** Resources, Discussion. **Fred Beisson:** Conceptualization, Supervision, Methodology, Validation, Writing - review & editing. **Damien Sorigué:** Conceptualization, Methodology, Validation, Resources, Supervision, Project administration, Funding acquisition, Writing - review & editing. All the authors read and approved the final version of the manuscript.

Please cite this article as: Baca-Porcel Á., Samire P.P., Legeret B., Auroy-Tarrago P., Veillet F., Giacalone C., Cuine S., Moulin S., Peltier G., Li-Beisson Y., Beisson F., Sorigué D. Microbial photoproduction of *n*-heptane. Biofuel Research Journal 47 (2025) 2470-2486. DOI: 10.18331/BRJ2025.12.3.3.

Conflict of interest

The authors declare that they have no conflicts of interest to disclose.

References

[1] Akhtar, M.K., Turner, N.J., Jones, P.R., 2013. Carboxylic acid reductase is a versatile enzyme for the conversion of fatty acids into fuels and chemical commodities. Proc. Natl. Acad. Sci. U. S. A. 110(1), 87-92.

[2] Amer, M., Hoeven, R., Kelly, P., Faulkner, M., Smith, M.H., Toogood, H.S., Scrutton, N.S., 2020a. Renewable and tuneable bio-LPG blends derived from amino acids. Biotechnol. Biofuels. 13(1), 125.

[3] Amer, M., Wojcik, E.Z., Sun, C., Hoeven, R., Hughes, J.M.X., Faulkner, M., Yunus, I.S., Tait, S., Johannissen, L.O., Hardman, S.J.O., Heyes, D.J., Chen, G.-Q., Smith, M.H., Jones, P.R., Toogood, H.S., Scrutton, N.S., 2020b. Low carbon strategies for sustainable bio-alkane gas production and renewable energy. Energy Environ. Sci. 13(6), 1818-1831.

[4] Aselmeyer, C., Légeret, B., Bénarouche, A., Sorigué, D., Parsiegla, G., Beisson, F., Carrière, F., 2021. Fatty acid photodecarboxylase is an interfacial enzyme that binds to lipid-water interfaces to access its insoluble substrate. Biochemistry. 60(42), 3200-3212.

[5] Blazeck, J., Liu, L., Knight, R., Alper, H.S., 2013. Heterologous production of pentane in the oleaginous yeast *Yarrowia lipolytica*. J. Biotechnol. 165(3-4), 184-194.

[6] Bruder, S., Moldenhauer, E.J., Lemke, R.D., Ledesma-Amaro, R., Kabisch, J., 2019. Drop-in biofuel production using fatty acid photodecarboxylase from *Chlorella variabilis* in the oleaginous yeast *Yarrowia lipolytica*. Biotechnol. Biofuels. Bioprod. 12(1), 202.

[7] Burlacot, A., Burlacot, F., Li-Beisson, Y., Peltier, G., 2020. Membrane inlet mass spectrometry: a powerful tool for algal research. Front. Plant Sci. 11, 1302.

[8] Cao, Y.X., Xiao, W.H., Zhang, J.L., Xie, Z.X., Ding, M.Z., Yuan, Y.J., 2016. Heterologous biosynthesis and manipulation of alkanes in *Escherichia coli*. Metab. Eng. 38, 19-28.

[9] Chanquia, S.N., Benfeldt, F.V., Petrovai, N., Santner, P., Hollmann, F., Eser, B.E., Kara, S., 2022. Immobilization and application of fatty acid photodecarboxylase in deep eutectic solvents. Chembiochem. 23(23), e202200482.

[10] Chanquia, S.N., Vernet, G., Kara, S. 2021. Photobioreactors for cultivation and synthesis: specifications, challenges, and perspectives. Eng. Life Sci. 22, 712-724.

[11] Cheng, F., Li, H., Wu, D.Y., Li, J.M., Fan, Y., Xue, Y.P., Zheng, Y.G., 2020. Light-driven deracemization of phosphinothricin by engineered fatty acid photodecarboxylase on a gram scale. Green Chem. 22(20), 6815-6818.

[12] Choi, Y.J., Lee, S.Y., 2013. Microbial production of short-chain alkanes. Nature. 502(7472), 571-574.

[13] Crépin, L., Barthe, M., Leray, F., Guillouet, S.E., 2018. Alka(e)ne synthesis in *Cupriavidus necator* boosted by the expression of endogenous and heterologous ferredoxin-ferredoxin reductase systems. Biotechnol. Bioeng. 115(10), 2576-2584.

[14] Crépin, L., Lombard, E., Guillouet, S.E., 2016. Metabolic engineering of *Cupriavidus necator* for heterotrophic and autotrophic alka(e)ne production. Metab. Eng. 37, 92-101.

[15] Dehesh, K., Jones, A., Knutzon, D.S., Voelker, T.A., 1996. Production of high levels of 8:0 and 10:0 fatty acids in transgenic canola by overexpression of *Ch FatB2*, a thioesterase cDNA from *Cuphea hookeriana*. Plant J. 9(2), 167-172.

[16] Emmanuel, M.A., Bender, S.G., Bilodeau, C., Carceller, J.M., DeHovitz, J.S., Fu, H., Liu, Y., Nicholls, B.T., Ouyang, Y., Page, C.G., Qiao, T., Raps, F.C., Sorigué, D.R., Sun, S.Z., Turek-Herman, J., Ye, Y., Rivas-Souchet, A., Cao, J., Hyster, T.K., 2023. Photobiocatalytic strategies for organic synthesis. Chem. Rev. 123(9), 5459-5520.

[17] Fatma, Z., Hartman, H., Poolman, M.G., Fell, D.A., Srivastava, S., Shakeel, T., Yazdani, S.S., 2018. Model-assisted metabolic engineering of *Escherichia coli* for long chain alkane and alcohol production. Metab. Eng. 46, 1-12.

[18] Geng, J., Liao, P., Tan, G.Y.A., Zhu, F.Y., Pradhan, N., 2023. Opportunities and challenges for n-alkane and n-alkene biosynthesis: a sustainable microbial biorefinery. Biofuel Res. J. 10(4), 1974-1988.

[19] Gil, A., Sancho-Sanz, I., Korili, S. A., 2024. Progress and perspectives in the catalytic hydrotreatment of bio-oils: effect of the nature of the metal catalyst. Ind. Eng. Chem. Res. 63(27), 11759-11775.

[20] Herman, N.A., Zhang, W., 2016. Enzymes for fatty acid-based hydrocarbon biosynthesis. Curr. Opin. Chem. Biol. 35, 22-28.

[21] Hernández Lozada, N.J., Lai, R.Y., Simmons, T.R., Thomas, K.A., Chowdhury, R., Maranas, C.D., Pfleger, B.F., 2018. Highly active C8-acyl-ACP thioesterase variant isolated by a synthetic selection strategy. ACS Synth. Biol. 7(9), 2205-2215.

[22] Huijbers, M.M.E., Zhang, W., Tonin, F., Hollmann, F., 2018. Light-driven enzymatic decarboxylation of fatty acids. Angew. Chem. Int. Ed Engl. 57(41), 13648-13651.

[23] Jaroensuk, J., Intasian, P., Wattanasuepsin, W., Akeratchatapan, N., Kesornpun, C., Kittipanukul, N., Chaiyen, P., 2020. Enzymatic reactions and pathway engineering for the production of renewable hydrocarbons. J. Biotechnol. 309, 1-19.

[24] Jiménez-Díaz, L., Caballero, A., Pérez-Hernández, N., Segura, A., 2017. Microbial alkane production for jet fuel industry: motivation, state of the art and perspectives. Microb. Biotechnol. 10(1), 103-124.

[25] Jing, F., Cantu, D.C., Tvaruzkova, J., Chipman, J.P., Nikolau, B.J., Yandeau-Nelson, M.D., Reilly, P.J., 2011. Phylogenetic and experimental characterization of an acyl-ACP thioesterase family reveals significant diversity in enzymatic specificity and activity. BMC Biochem. 12(1), 44.

[26] Klüh, D., Waldmüller, W., Gaderer, M., 2021. Kolbe electrolysis for the conversion of carboxylic acids to valuable products-a process design study. Clean Technol. 3(1), 1-18.

[27] Kuppusamy, S., Maddela, N.R., Megharaj, M., Venkateswarlu, K., 2019. Total petroleum hydrocarbons: environmental fate, toxicity, and remediation, 2020th ed. Springer Nature, Cham, Switzerland.

[28] Lakavath, B., Hedison, T.M., Heyes, D.J., Shanmugam, M., Sakuma, M., Hoeven, R., Tilakaratna, V., Scrutton, N.S., 2020. Radical-based photoinactivation of fatty acid photodecarboxylases. Anal. Biochem. 600, 113749.

[29] Lee, S.B., Suh, M.C., 2013. Recent advances in cuticular wax biosynthesis and its regulation in *Arabidopsis*. Mol. Plant. 6(2), 246-249.

[30] Li, D., Han, T., Xue, J., Xu, W., Xu, J., Wu, Q., 2021. Engineering fatty acid photodecarboxylase to enable highly selective decarboxylation of *trans* fatty acids. Angew. Chem. Int. Ed. Engl. 60(38), 20695-20699.

[31] Li, F., Xia, A., Guo, X., Huang, Y., Zhu, X., Zhu, X., Liao, Q., 2023. Immobilization of fatty acid photodecarboxylase in magnetic nickel ferrite nanoparticle. Bioresour. Technol. 385, 129374.

[32] Li, J., Ma, Y., Liu, N., Eser, B.E., Guo, Z., Jensen, P.R., Stephanopoulos, G., 2020. Synthesis of high-titer alka(e)nes in *Yarrowia lipolytica* is enabled by a discovered mechanism. Nat. Commun. 11(1), 6198.

[33] Ma, Y., Zhong, X., Wu, B., Lan, D., Zhang, H., Hollmann, F., Wang, Y., 2023. A photodecarboxylase from *Micractinium conductrix* active on medium and short-chain fatty acids. Chin. J. Catal. 44, 160-170.

[34] Moulin, S., Légeret, B., Blangy, S., Sorigué, D., Burlacot, A., Auroy, P., Li-Beisson, Y., Peltier, G., Beisson, F., 2019. Continuous photoproduction of hydrocarbon drop-in fuel by microbial cell factories. Sci. Rep. 9(1), 13713.

[35] Moulin, S.L.Y., Beyly-Adriano, A., Cuiné, S., Blangy, S., Légeret, B., Floriani, M., Burlacot, A., Sorigué, D., Samire, P.P., Li-Beisson, Y., Peltier, G., Beisson, F., 2021. Fatty acid photodecarboxylase is an ancient photoenzyme that forms hydrocarbons in the thylakoids of algae. Plant Physiol. 186(3), 1455-1472.

[36] Niederer, M., Stebler, T., Grob, K., 2016. Mineral oil and synthetic hydrocarbons in cosmetic lip products. Int. J. Cosmet. Sci. 38(2), 194-200.

[37] Ohlendorf, R., Vidavski, R.R., Eldar, A., Moffat, K., Möglich, A., 2012. From dusk till dawn: one-plasmid systems for light-regulated

Please cite this article as: Baca-Porcel Á., Samire P.P., Legeret B., Auroy-Tarrago P., Veillet F., Giacalone C., Cuine S., Moulin S., Peltier G., Li-Beisson Y., Beisson F., Sorigué D. Microbial photoproduction of *n*-heptane. Biofuel Research Journal 47 (2025) 2470-2486. DOI: 10.18331/BRJ2025.12.3.3.

gene expression. J. Mol. Biol. 416(4), 534-542.
[38] Ohlrogge, J., Thrower, N., Mhaske, V., Stymne, S., Baxter, M., Yang, W., Liu, J., Shaw, K., Shorrosh, B., Zhang, M., Wilkerson, C., Matthäus, B., 2018. PlantFAdb: a resource for exploring hundreds of plant fatty acid structures synthesized by thousands of plants and their phylogenetic relationships. Plant J. 96(6), 1299-1308.
[39] Rossbach, B., Kegel, P., Letzel, S., 2012. Application of headspace solid phase dynamic extraction gas chromatography/mass spectrometry (HS-SPDE-GC/MS) for biomonitoring of n-heptane and its metabolites in blood. Toxicol. Lett. 210(2), 232-239.
[40] [Rui, Z., Harris, N.C., Zhu, X., Huang, W., Zhang, W., 2015. Discovery of a family of desaturase-like enzymes for 1-alkene biosynthesis. ACS Catal. 5(12), 7091-7094.
[41] Samire, P.P., Zhuang, B., Légeret, B., Baca-Porcel, Á., Peltier, G., Sorigué, D., Aleksandrov, A., Beisson, F., Müller, P., 2023. Autocatalytic effect boosts the production of medium-chain hydrocarbons by fatty acid photodecarboxylase. Sci. Adv. 9(13), eadg3881.
[42] Schirmer, A., Rude, M.A., Li, X., Popova, E., del Cardayre, S.B., 2010. Microbial biosynthesis of alkanes. Science. 329(5991), 559-562.
[43] Smagala, T. G., Christensen, E., Christison, K. M., Mohler, R. E., Gjersing, E., McCormick, R. L., 2013. Hydrocarbon renewable and synthetic diesel fuel blendstocks: composition and properties. Energy Fuels. 27(1), 237-246.
[44] Sorigué, D., Hadjidemetriou, K., Blangy, S., Gotthard, G., Bonvalet, A., Coquelle, N., Samire, P., Aleksandrov, A., Antonucci, L., Benachir, A., Boutet, S., Byrdin, M., Cammarata, M., Carbajo, S., Cuiné, S., Doak, R.B., Foucar, L., Gorel, A., Grünbein, M., Hartmann, E., Hienerwadel, R., Hilpert, M., Kloos, M., Lane, T.J., Légeret, B., Legrand, P., Li-Beisson, Y., Moulin, S.L.Y., Nurizzo, D., Peltier, G., Schirò, G., Shoeman, R.L., Sliwa, M., Solinas, X., Zhuang, B., Barends, T.R.M., Colletier, J.P., Joffre, M., Royant, A., Berthomieu, C., Weik, M., Domratcheva, T., Brettel, K., Vos, M.H., Schlichting, I., Arnoux, P., Müller, P., Beisson, F., 2021. Mechanism and dynamics of fatty acid photodecarboxylase. Science. 372(6538), eabd5687.
[45] Sorigué, D., Légeret, B., Cuiné, S., Blangy, S., Moulin, S., Billon, E., Richaud, P., Brugière, S., Couté, Y., Nurizzo, D., Müller, P., Brettel, K., Pignol, D., Arnoux, P., Li-Beisson, Y., Peltier, G., Beisson, F., 2017. An algal photoenzyme converts fatty acids to hydrocarbons. Science. 357(6354), 903-907.
[46] Spacey, H.J., Healy, D., Kalapothakis, J.M.D., Ma, J., Sakuma, M., Barran, P.E. Heyes, D.J., Scrutton, N.S., 2025. Exploring the increased activity of the blue light-dependent photoenzyme fatty acid photodecarboxylase under violet light. ACS Catal. 15(8), 6088-6097.
[47] Teimouri, Z., Abatzoglou, N., Dalai, A. K., 2021. Kinetics and selectivity study of Fischer-Tropsch synthesis to C_5+ hydrocarbons: a review. Catalysts. 11(3), 330.
[48] Vignesh, P., Kumar, A. R. P., Ganesh, N. S., Jayaseelan, V., Sudhakar, K., 2021. Biodiesel and green diesel generation: an overview. Oil Gas Sci. Technol. Rev. IFP Energies Nouvelles. 76, 6.
[49] Wu, Y., Paul, C.E., Hollmann, F., 2021. Stabilisation of the fatty acid decarboxylase from *Chlorella variabilis* by caprylic acid. Chembiochem. 22(14), 2420-2423.
[50] Yang, K., Qiao, Y., Li, F., Xu, Y., Yan, Y., Madzak, C., Yan, J., 2019. Subcellular engineering of lipase dependent pathways directed towards lipid related organelles for highly effectively compartmentalized biosynthesis of triacylglycerol derived products in *Yarrowia lipolytica*. Metab. Eng. 55, 231-238.
[51] Yan, H., Wang, Z., Wang, F., Tan, T., Liu, L., 2016. Biosynthesis of chain-specific alkanes by metabolic engineering in *Escherichia coli*. Eng. Life Sci. 16(1), 53-59.
[52] Yunus, I.S., Anfelt, J., Sporre, E., Miao, R., Hudson, E.P., Jones, P.R., 2022. Synthetic metabolic pathways for conversion of CO_2 into secreted short-to medium-chain hydrocarbons using cyanobacteria. Metab. Eng. 72, 14-23.
[53] Yunus, I.S., Wichmann, J., Wördenweber, R., Lauersen, K.J., Kruse, O., Jones, P.R., 2018. Synthetic metabolic pathways for photobiological conversion of CO_2 into hydrocarbon fuel. Metab. Eng. 49, 201-211.
[54] Zeng, Y., Yin, X., Liu, L., Zhang, W., Chen, B., 2022. Comparative characterization and physiological function of putative fatty acid photodecarboxylases. Mol. Catal. 532, 112717.
[55] Zhang, W., Lee, J.H., Younes, S.H.H., Tonin, F., Hagedoorn, P.L., Pichler, H., Baeg, Y., Park, J.B., Kourist, R., Hollmann, F., 2020. Photobiocatalytic synthesis of chiral secondary fatty alcohols from renewable unsaturated fatty acids. Nat. Commun. 11(1), 2258.
[56] Zhang, W., Ma, M., Huijbers, M.M.E., Filonenko, G.A., Pidko, E.A., van Schie, M., de Boer, S., Burek, B.O., Bloh, J.Z., van Berkel, W.J.H., Smith, W.A., Hollmann, F., 2019. Hydrocarbon synthesis via photoenzymatic decarboxylation of carboxylic acids. J. Am. Chem. Soc. 141(7), 3116-3120.

Ángel Baca-Porcel is a Ph.D. student in the EBMP (Environment, Bioenergies, Microalgae, and Plants) research team at the Institute of Biosciences and Biotechnologies of Aix-Marseille (BIAM), part of the French Alternative Energies and Atomic Energy Commission (CEA) in Cadarache, France. He holds a Master's degree in Biology and Health (specializing in Microbiology) from the University of Paris-Saclay, France, and a Bachelor's degree in Biochemistry from the University of Granada, Spain. His research interests include hydrocarbon-forming enzymes, lipid metabolism and biochemistry, as well as metabolic engineering for the production of valuable bioproducts. His ResearchGate profile can be found at the following link: https://www.researchgate.net/profile/Angel-Baca-Porcel-2

Dr. Poutoum Palakiyém SAMIRE is a postdoctoral Researcher in the EBMP (Environment, Bioenergies, Microalgae, and Plants) research team at the Institute of Biosciences and Biotechnologies of Aix-Marseille (BIAM), part of the French Alternative Energies and Atomic Energy Commission (CEA) in Cadarache, France. With a PhD in biotechnology from Aix-Marseille University, Poutoum is particularly interested in the use of biocatalysis to produce biosourced molecules of industrial interest. His research profile on Google Scholar can be found at the following link:
https://scholar.google.fr/citations?user=Hwb0QegAAAAJ&hl=fr

Please cite this article as: Baca-Porcel Á., Samire P.P., Legeret B., Auroy-Tarrago P., Veillet F., Giacalone C., Cuine S., Moulin S., Peltier G., Li-Beisson Y., Beisson F., Sorigué D. Microbial photoproduction of *n*-heptane. Biofuel Research Journal 47 (2025) 2470-2486. DOI: 10.18331/BRJ2025.12.3.3.

Bertrand Légéret is an engineer at the CNRS specializing in mass spectrometry. He holds a master's degree in organic chemistry from the University of Orléans, France, and a master's degree in analytical chemistry from the University of Rennes, France. For ten years, he led the mass spectrometry platform of the chemistry department at Clermont-Ferrand University, France. Since 2012, he has been the technical manager of the Heliobiotec platform from BIAM, France. His skills include lipidomics, analytical chemistry, biocatalysis, and lipid metabolism. His research profile on Google Scholar can be found at the following link: https://scholar.google.com/citations?hl=enuser=982fYx8AAAAJ&user=982fYx8AAAAJ

Dr. Florian Veillet is a researcher in the EBMP (Environment, Bioenergies, Microalgae, and Plants) research team at the Institute of Biosciences and Biotechnologies of Aix-Marseille (BIAM), part of the French Alternative Energies and Atomic Energy Commission (CEA) in Cadarache, France. He holds a PhD in plant biology and molecular genetics. His research interests mainly focus on deciphering the lipid and sugar metabolisms in a wide range of algae.

Pascaline Auroy is a technician in the EBMP (Environment, Bioenergies, Microalgae, and Plants) research team at the Institute of Biosciences and Biotechnologies of Aix-Marseille (BIAM), part of the French Alternative Energies and Atomic Energy Commission (CEA) in Cadarache, France. She has a university technician degree in biology (option agronomy) from Université of Auvergne, France. She specialized in molecular biology, cloning tools, techniques, and genome editing. Her research profile on Google Scholar can be found at the following link: https://pubmed.ncbi.nlm.nih.gov/?cmd=search&term=Pascaline%20Auroy&page=2

Cécile Giacalone is a technician in the EBMP (Environment, Bioenergies, Microalgae, and Plants) research team at the Institute of Biosciences and Biotechnologies of Aix-Marseille (BIAM), part of the French Alternative Energies and Atomic Energy Commission (CEA) in Cadarache, France.

Stéphan Cuiné is an engineer in the EBMP (Environment, Bioenergies, Microalgae, and Plants) research team at the Institute of Biosciences and Biotechnologies of Aix-Marseille (BIAM), part of the French Alternative Energies and Atomic Energy Commission (CEA) in Cadarache, France.

Dr. Solène Moulin is a postdoctoral researcher at Stanford University, California, USA. She received a Ph.D. degree in cellular and molecular biology from Aix-Marseille University in 2019 for her research on the production of hydrocarbons in microalgae and biotechnological applications. Her current research focuses on symbiosis with nitrogen-fixing microbes and their biotechnological application for sustainability. Her research profile on Google Scholar can be found at the following link:
https://scholar.google.com/citations?user=0IpaS7sAAAAJ&hl=fr&oi=ao

Dr. Gilles Peltier is a leading expert in the field of microalgal photosynthesis. Over the years, he has developed an integrative research approach combining genetics, physiology, and biophysics to elucidate novel mechanisms regulating photosynthesis in microalgae. He has been a pioneer in exploring alternative electron transport pathways. He has cultivated a strong research focus on the potential of microalgae as a sustainable source of bioenergy. Dr. Peltier has authored more than 140 peer-reviewed publications and holds an h-index of 61. His research profile on Google Scholar can be found at the following link: https://scholar.google.fr/citations?user=AOU9nLUAAAAJ&hl=en

Dr. Yonghua Li-Beisson is a biologist specializing in lipid metabolism. She obtained a PhD on lipid metabolism in oleaginous filamentous fungi (Colin Ratledge's laboratory, U.K.), where her work highlighted the importance of reducing power (via the malic enzyme) in the stimulation of de novo fatty acid biosynthesis. She then did postdoctoral research in the laboratory of John Ohlrogge (MSU, USA), where she studied lipid metabolism in the plant Arabidopsis thaliana. At CEA Cadarache, she focused on the study of photosynthetic carbon metabolism in microalgae. Her general objectives are to understand the molecular mechanisms of the conversion of light energy into chemical energy contained in microalgae storage compounds such as lipids and starch. In particular, she is interested in the subcellular energetics and compartmentalization that govern CO2 capture and carbon flux into fatty acids and stored as lipid droplets. In addition to research, she serves as a member of the editorial board for the Plant Cell, Plant Cell and Physiology, and Progress in Lipid Research. She serves on the advisory board for New Phytologist. She is leading the team focusing on algal photosynthesis, nutrient sensing, and metabolism, and she also leads the European platform HelioBiotec. Her research profile on Google Scholar can be found at the following link:
https://scholar.google.com/citations?user=v2Y3s9EAAAAJ&hl=en

Dr. Fred Beisson is a CNRS research director based in Cadarache in southern France. He obtained a PhD in Biochemistry from Aix-Marseille University in 1999. He completed a postdoctoral fellowship with John Ohlrogge at Michigan State University. His primary research interests lie in discovering enzymes involved in lipid metabolism in plants and algae, as well as their biotechnological applications. He is currently working on the biosynthesis of hydrocarbons derived from fatty acids. His research profile on Google Scholar can be found at the following link: https://scholar.google.com/citations?user=o6mUuxUAAAAJ&hl=en

Please cite this article as: Baca-Porcel Á., Samire P.P., Legeret B., Auroy-Tarrago P., Veillet F., Giacalone C., Cuine S., Moulin S., Peltier G., Li-Beisson Y., Beisson F., Sorigué D. Microbial photoproduction of *n*-heptane. Biofuel Research Journal 47 (2025) 2470-2486. DOI: 10.18331/BRJ2025.12.3.3.

Dr. Damien Sorigué is a researcher in the EBMP (Environment, Bioenergies, Microalgae, and Plants) team at the Institute of Biosciences and Biotechnologies of Aix-Marseille (BIAM), part of the French Alternative Energies and Atomic Energy Commission (CEA) in Cadarache, France. He holds a Ph.D. in Biochemistry from Aix-Marseille University and recently completed a Marie Skłodowska-Curie Global Fellowship on photobiocatalysis with Prof. Todd K. Hyster at Cornell and Princeton Universities (USA). His research focuses on the discovery, characterization, and engineering of photoenzymes, particularly fatty acid photodecarboxylase (FAP), to enable light-driven biocatalysis for sustainable biofuel production and green chemical transformations. His research profile on Google Scholar can be found at the following link: https://scholar.google.com/citations?user=E-kWN_kAAAAJ&hl=fr

Please cite this article as: Baca-Porcel Á., Samire P.P., Legeret B., Auroy-Tarrago P., Veillet F., Giacalone C., Cuine S., Moulin S., Peltier G., Li-Beisson Y., Beisson F., Sorigué D. Microbial photoproduction of *n*-heptane. Biofuel Research Journal 47 (2025) 2470-2486. DOI: 10.18331/BRJ2025.12.3.3.

Supplementary Information

Table S1.
Protein sequences of all genes heterologously expressed in *E. coli* in this study.

Protein	Amino Acid Sequence (N-Terminal to C-Terminal) in FASTA Format
***Cv*FAP**	MGHHHHHHSSGVDLGTENLYFQSMASAVEDIRKVLSDSSSPVAGQKYDYILVGGGTAACVLANRLSADGSKRVLVLEAGPDNTSRDVKIPAAITRLFRSPLDWNLF SELQEQLAERQIYMARGRLLGGSSATNATLYHRGAAGDYDAWGVEGWSSEDVLSWFVQAETNADFGPGAYHGSGGPMRVENPRYTNKQLHTAFFKAAEEVGLT PNSDFNDWSHDHAGYGTFQVMQDKGTRADMYRQYLKPVLGRRNLQVLTGAAVTKVNIDQAAGKAQALGVEFSTDGPTGERLSAELAPGGEVIMCAGAVHTPFL LKHSGVGPSAELKEFGIPVVSNLAGVGQNLQDQPACLTAAPVKEKYDGIAISDHIYNEKGQIRKRAIASYLLGGRGGLTSTGCDRGAFVRTAGQALPDLQVRFVPG MALDPDGVSTYVRFAKFQSQGLKWPSGITMQLIACRPQSTGSVGLKSADPFAPPKLSPGYLTDKDGADLATLRKGIHWARDVARSSALSEYLDGELFPGSGVVSDD QIDEYIRRSIHSSNAITGTCKMGNAGDSSSVVDNQLRVHGVEGLRVVDASVVPKIPGGQTGAPVVMIAERAAALLTGKATIGASAAAPATVAA
TrxA-*Cv*FAP	MGHHHHHHSDKIIHLTDDSFDTDVLKADGAILVDFWAEWCGPCKMIAPILDEIADEYQGKLTVAKLNIDQNPGTAPKYGIRGIPTLLLFKNGEVAATKVGALSKGQ LKEFLDANLAGSGSGVSGVDLGTENLYFQSASAVEDIRKVLSDSSSPVAGQKYDYILVGGGTAACVLANRLSADGSKRVLVLEAGPDNTSRDVKIPAAITRLFRSPL DWNLFSELQEQLAERQIYMARGRLLGGSSATNATLYHRGAAGDYDAWGVEGWSSEDVLSWFVQAETNADFGPGAYHGSGGPMRVENPRYTNKQLHTAFFKAAE EVGLTPNSDFNDWSHDHAGYGTFQVMQDKGTRADMYRQYLKPVLGRRNLQVLTGAAVTKVNIDQAAGKAQALGVEFSTDGPTGERLSAELAPGGEVIMCAGAV HTPFLLKHSGVGPSAELKEFGIPVVSNLAGVGQNLQDQPACLTAAPVKEKYDGIAISDHIYNEKGQIRKRAIASYLLGGRGGLTSTGCDRGAFVRTAGQALPDLQVR FVPGMALDPDGVSTYVRFAKFQSQGLKWPSGITMQLIACRPQSTGSVGLKSADPFAPPKLSPGYLTDKDGADLATLRKGIHWARDVARSSALSEYLDGELFPGSGV VSDDQIDEYIRRSIHSSNAITGTCKMGNAGDSSSVVDNQLRVHGVEGLRVVDASVVPKIPGGQTGAPVVMIAERAAALLTGKATIGASAAAPATVAA
TrxA-*Cr*FAP	MGHHHHHHSDKIIHLTDDSFDTDVLKADGAILVDFWAEWCGPCKMIAPILDEIADEYQGKLTVAKLNIDQNPGTAPKYGIRGIPTLLLFKNGEVAATKVGALSKGQ LKEFLDANLAGSGSGVSGVDLGTENLYFQSMEVAVPAGITRLFAHPVMDWGMSSLTQKQLVAREIYLARGRMLGGSSGSNATLYHRGSAADYDAWGLEGWSSK DVLDWFVKAECYADGPKPYHGTGGSMNTEQPRYENVLHDEFFKAAAATGLPANPDFNDWSHPQDGFGEFQVSQKKGQRADTYRTYLKPAMARGNLKVVIGAR ATKVNIEKGSSGARTTGVEYAMQQFGDRFTAELAPGGEVLMCSGAVHTPHLLMLSGVGPAATLKEHGIDVVSDLSGVGQNLQDHPAAVLAARAKPEFEKLSVTSE VYDDKCNIKLGAVAQYLFQRRGPLATTGCDHGAFVRTSSSLSQPDLQMRFVPGCALDPDGVKSYIVFGELKKQGRAWPGGITLQLLAIRAKSKGSIGLKAADPFINP AININYFSDPADLATLVNAVKMARKIAAQEPLKKYLQEETFPGERASSDKDLEEYIRRTVHSGNALVGTAAMGASPAAGAVVSSADLKVFGVEGLRVVDASVLPRI PGGQTGAATVMVAERAAALLRGQATIAPSRQPVAV
TrxA-*Cc*FAP	MGHHHHHHSDKIIHLTDDSFDTDVLKADGAILVDFWAEWCGPCKMIAPILDEIADEYQGKLTVAKLNIDQNPGTAPKYGIRGIPTLLLFKNGEVAATKVGALSKGQ LKEFLDANLAGSGSGVSGVDLGTENLYFQSSSEAATTYDYIIVGGGAAGCVLANRLTEDPSTRVLLLEAGKPDDSFYLHVPLGFPYLLGSPNDWAFVTEPEPNLANR RLYFPRGKVLGGSHAISVMLYHRGHPADYTAWAESAPGWAPQDVLPYFLKSESQQSAVPNQDAHGYEGPLAVSDLARLNPMSKAFIKAAHNAAGLNHNPDFND WATGQDGVGPFQVTQRDGSRESPATSYLRAAKGRRNLTVMTGAVVERILFENPAGSSTPVATAVSFIDSKGTRVRMSASREILLCGGVYATPQLLMLSGVGPAEHL RSHGIEIVADVPAVGQNLQDHAAAMVSFESQNPEKDKANSSVYYTERTGKNIGTLLNYVFRGKGPLTSPMCEAGGFAKTDPSMDACDLQLRFIPFVSEPDPYHSLA DFATAGSYLQNRANRPTGFTIQSVAARPKSRGHVQLRSTDVRDSMSIHGNWISNDADLKTLVHGVKLCRTIGNDDSMKEFRGRELYPGGEKVSDADIEAYIRDTCH TANAMVGTCRMGIGEQAAVDPALQVKGVARLRVVDSSVMPTLPGGQSGAPTMMIAEKGADLIRAAARQADAATVGAAA
TrxA-*Gs*FAP	MGHHHHHHSDKIIHLTDDSFDTDVLKADGAILVDFWAEWCGPCKMIAPILDEIADEYQGKLTVAKLNIDQNPGTAPKYGIRGIPTLLLFKNGEVAATKVGALSKGQ LKEFLDANLAGSGSGVSGVDLGTENLYFQSGFDRSREFDYVIVGGGAAGCVLASRLSEDKRSTVLLLEAGKEDENFYIHVPMGFPYLVGSDLDWKYQSTSEERLLD RKIMWPRGKVLGGSHAISVMLYLRGSANDYREWERCGALGWGPEDVLPYYLKAENNLRGVGPYHGKGGPLTVSDLPSPNEMSHAFVIAGQTLDIPYNKDFNDWS HSQEGIGLFQVTQANGKRVSPATAYLHPVRSRRNLFIETQRHVEKILFTKEIGSCPRAIGVSYINSNGKRERAMIRKEVVVSAGAYGSPQLLMLSGIGPSNVLDSIGIPT VMPLEGVGKNLQDHFAVMFSCKSPDPSKDRKRRNLYYTDDTGKDWKTILTWFLSGKGPLTSTMCEAGAFLKTNPIFNDPDLQLRFIPFFSEADPYFSLSDYSSKGMF FKNRSHRPSGFTIQSVAIRPKSRGRLTIQSKDPRMLPIIESGWFSSQEDLETLLRGISLSQKLVHASPLASYFGEQCFPSTGLSKKEDIIRYISSTCHTANAVVGTCRMGT DKQAVVNPNLQVMGVERLRVLLQL
TrxA-*Es*FAP	MGHHHHHHSDKIIHLTDDSFDTDVLKADGAILVDFWAEWCGPCKMIAPILDEIADEYQGKLTVAKLNIDQNPGTAPKYGIRGIPTLLLFKNGEVAATKVGALSKGQ LKEFLDANLAGSGSGVSGVDLGTENLYFQSSMSVAEEGHKFIIIGGGTAGCVLANRLSADKDNSVLVLEAGSEKFNDRNIKMPIAILRLFKSVFDWGFQSENEKFAT GDGIYLCRGKVLGGSSCTNVMLYHRGEEADYDAWGVDGWKGKDVLPYFKKAENNRSKKKGEFHGKGGLMQVENARYMNPLTKLFFKACEQAGLSENEDFND WSHSQEGFGRFQVAQKRGKRCSAASSYLKEAMGRKNLDVQTSAQITKVLIENGGAIGVEYVRDGEKKIAKLAVGGEILLAGGAISSPQVLMLSGVGPAEHLRSKGI EVKSNVPGVGKNLRDHPAVTVMADINKPISITDKVLKEGSGDVNKITALQWLLTGTGPLTSPGCENGAFFKTTPDKAAADLQLRFVPGRSTTPDGVKAYNTIGTKG RPPSGVTVQVVGIRPQSEGHVELRSSDPFDKPHIVTNYLESGEDMASLTNGIEMARKLFDQEAFGEMVDKEVFPGRDNKEISEYIKSTVHSANALVGTCKMGEESDN MSVVNSALKVKGVAGLRVIDSSVMPSIPGGQTAAPTIMIAEKAADMLMA
TrxA-*Ng*FAP	MGHHHHHHSDKIIHLTDDSFDTDVLKADGAILVDFWAEWCGPCKMIAPILDEIADEYQGKLTVAKLNIDQNPGTAPKYGIRGIPTLLLFKNGEVAATKVGALSKGQ LKEFLDANLAGSGSGVSGVDLGTENLYFQSLQSVSMKAPAAVASSTYDYIIVGGGIGGCVLANRLTESGRFKVLLLEAGKSAERNPYVNIPAGVVRLFKSALDWQF ESAPERHLDGKEVYLVRGKAMGGSSAVNVMLVHRGSASDYAKWEAEGAQGWGPEEALRYFKKMEDNLVGGEGRWHGQGGMYPVDDVKYQNPLSKRFLQACE EYGWRANPDFNDWSHPQDGYGSFKVAQKHGKRVTAASGYLNKAVRRRPNLDILSEALVTRVLLEGEGDVKAVGVEFTGKDGKTHQVRTTGKAGEVLLAGGAV NSPQLLMLSGIGPEADLQAVGIATKVNRPGVGENLQDHPAVTIAHNITRPISLCDDLFLFHTPVPKPHQVLRWTLTGSGPLTTPGCDHGAFLKTREDLQEPNVQFRFI AGRGSDPDGVRSYIMGGSARPLSGLTLQVVNIRPKSKGKLTLASKDPLKKPRIEVRYLSAAEDLQALRTGMRIGRDLIKQRAFADILDEEVFPGPAAQTDEELDAYIR DSLHTANALVGTCKMGSVEDRNAVVDPECRVIGVGGLRVVDASVMPVIPGGQTGSGTTMLAEKAADLVRAHAGDLVEMGVQDEERKGGWFNGLLGRKQKVAT
TrxA-*At*TES	MGSSHHHHHHSSGLVPRGSHMASMTGGQQMGRIRMKFKKKFKIGRMHVDPFNYISMRYLVALMNEVAFDQAEILEKDIDMKNLRWIIYSWDIQIENNIRLGEEIEI TTIPTHMDKFYAYRDFIVESRGNILARAKATFLLMDITRLRPIKIPQNLSLAYGKENPIFDIYDMEIRNDLAFIRDIQLRRADLDNNFHINNAVYFDLIKETVDIYDKDIS YIKLIYRNEIRDKKQIQAFARREDKSIDFALRGEDGRDYCLGKIKTNV
***Cp*TES-287**	MGSSHHHHHHSSGLVPRGSHMASMTGGQQMGRIRMFDRKSKRPSMLMDSFGLERVVQDGLVFRQSFSIRSYEICADRTASMETVMNHVQETSLNQCKSIGLLDDG FGRSPEMCKRDLIWVVTRMKIMVNRYPTWGDTIEVSTWLSQSGKIGMGRDWLISDCNTGEILVRATSVYAMMNQKTRRFSKLPHEVRQEFAPHFLDSPPAIEDNDG KLQKFDVKTGDSIRKGLTPGWYDLDVNQHVSNVKYIGWILESMPTEVLETQELCSLTLEYRRECGRDSVLESVTSMDPSKVGDRFQYRHLLRLEDGADIMKGRTE WRPKNAGTNGAISTGKT
***Ch*TES**	MGSSHHHHHHSSGLVPRGSHMASMTGGQQMGRIRMVAAAASSAFFPVPAPGASPKPGKFGNWPSSLSPSFKPKSIPNGGFQVKANDSAHPKANGSAVSLKSGSLN TQEDTSSSPPPRTFLHQLPDWSRLLTAITTVFVKSKRPDMHDRKSKRPDMLVDSFGLESTVQDGLVFRQSFSIRSYEIGTDRTASIETLMNHLQETSLNHCKSTGILLD GFGRTLEMCKRDLIWVVIKMQIKVNRYPAWGDTVEINTRFSRLGKIGMGRDWLISDCNTGEILVRATSAYAMMNQKTRRLSKLPYEVHQEIVPLFVDSPVIEDSDL KVHKFKVKTGDSIQKGLTPGWNDLDVNQHVSNVKYIGWILESMPTEVLETQELCSLALEYRRECGRDSVLESVTAMDPSKVGVRSQYQHLLRLEDGTAIVNGATE WRPKNAGANGAISTGKTSNGNSVS

FAP variants were cloned without their native chloroplast transit peptide, His-tagged and either fused or not to TrxA. Color code: purple, His tag; red, TrxA; pink, TEV protease cleavage site; green, linker sequence.

Please cite this article as: Baca-Porcel Á., Samire P.P., Legeret B., Auroy-Tarrago P., Veillet F., Giacalone C., Cuine S., Moulin S., Peltier G., Li-Beisson Y., Beisson F., Sorigué D. Microbial photoproduction of *n*-heptane. Biofuel Research Journal 47 (2025) 2470-2486. DOI: 10.18331/BRJ2025.12.3.3.

Table S2.
Primer sequences used in this study.

Construction	Restriction Enzyme	Backbone	Insert	Primer	Sequence
pLIC03-*Cv*FAP	BsaI	pLIC03	*Cv*FAP gene	pLIC03-*Cv*FAP fw	ttggtctcccaatggccagcgcagttgaagatattcg
				pLIC03-*Cv*FAP rev	ttggtctcgtacttcatgctgcaacggttgccgg
pLIC07-*Cv*FAP	BsaI	pLIC07	*Cv*FAP gene	pLIC07-*Cv*FAP fw	ctgtacttccaatcagccagcgcagttgaagatattc
				pLIC07-*Cv*FAP rev	tatccacctttactgttatcatgctgcaacggttgccggtg
pDawn-*Cv*FAP	HindIII and XhoI	pDawn	*Cv*FAP gene fused with TrxA in 5' extremity	pDawn-*Cv*FAP fw	ttaagcttgagcgataaaattattcacctgactgacgac
				pDawn-*Cv*FAP rev	ttctcgagtcatgctgcaacggttgccggtg
pDawn-*Ch*TES	NheI and NotI	pDawn	*Ch*TES gene	*Ch*TES fw	cagccatatggctagcatgactggtggacagcaaatgggtcggatccgaatggttgcggccgcggccagc
				*Ch*TES rev	ttaaagtacgcggccgcttagctaacgctattgccattgctcgttttgcccgtgc
pDawn-*Ch*TES + *Cv*FAP	NotI and XhoI	pDawn-*Ch*TES	*Cv*FAP gene fused with TrxA and RBS in 5' extremity	*Ch*TES + *Cv*FAP fw	ttgcggccgcgtactttaactttaagaaggagatatac
				*Ch*TES + *Cv*FAP rev	ttctcgagtcatgctgcaacggttgccggtg
pDawn-*Cp*TES-287 + *Cv*FAP	NheI and NotI	pDawn-*Ch*TES + *Cv*FAP	*Cp*TES-287 gene	-	-
				-	-
pDawn-*At*TES + *Cv*FAP	NheI and NotI	pDawn-*Ch*TES + *Cv*FAP	*At*TES gene	-	-
				-	-
pDawn-*Cp*TES-*287*	NheI and NotI	pDawn-*Ch*TES	*CpTES-287 gene*	-	-
				-	-
pDawn-*At*TES	NheI and NotI	pDawn-*Ch*TES	AtTES *gene*	-	-

Synthetic genes *At*TES and *Cp*TES-287 were designed with NheI and NotI restriction sites at their 5' and 3' ends, respectively, to facilitate subcloning into expression vectors.

Please cite this article as: Baca-Porcel Á., Samire P.P., Legeret B., Auroy-Tarrago P., Veillet F., Giacalone C., Cuine S., Moulin S., Peltier G., Li-Beisson Y., Beisson F., Sorigué D. Microbial photoproduction of *n*-heptane. Biofuel Research Journal 47 (2025) 2470-2486. DOI: 10.18331/BRJ2025.12.3.3.

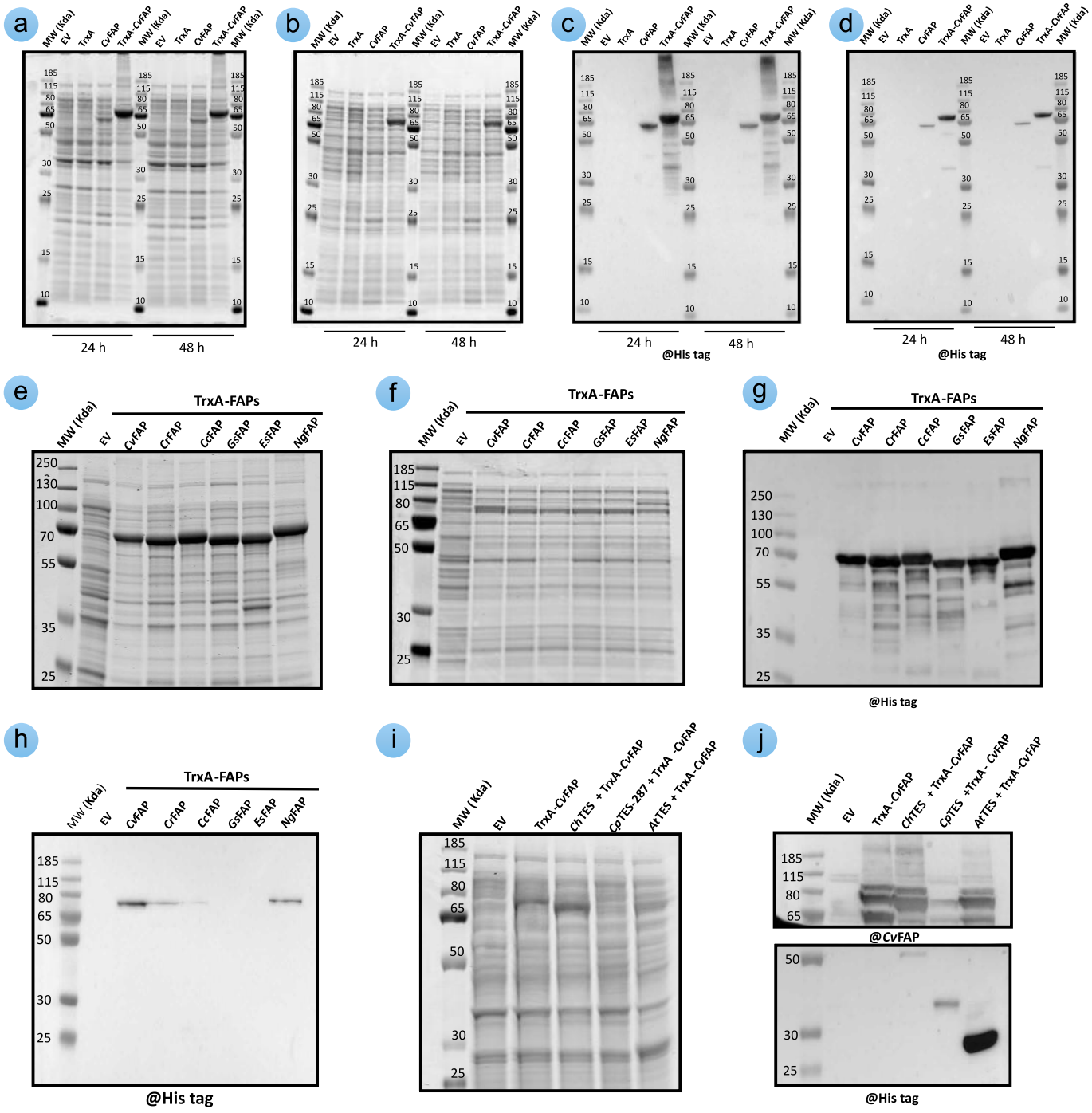

Fig. S1. SDS-PAGE and immunoblot analysis of *E. coli* strains co-expressing FAP homologs and/or different C8TESs. a–b) SDS-PAGE analysis of total (**a**) and soluble (**b**) proteins from strains expressing *Cv*FAP±TrxA fusion. **c–d**) Immunoblot detection of *Cv*FAP in total (**c**) and soluble (**d**) protein extracts. **e–f**) SDS-PAGE of total (**e**) and soluble (**f**) protein from strains expressing different FAP homologs after a 16-h induction period in the dark. **g–h**) Immunoblot detecting FAP homologs in (**g**) total and (**h**) soluble protein fraction. **i**) SDS-PAGE of total protein from strains co-expressing *Cv*FAP and different His-tagged C8TESs after an 18-h induction period. **j**) Immunoblots of total proteins from the same strains: *Cv*FAP (upper panel) and His-tagged C8TESs (lower panel). Protein loading was normalized based on cell density (OD600).

Please cite this article as: Baca-Porcel Á., Samire P.P., Legeret B., Auroy-Tarrago P., Veillet F., Giacalone C., Cuine S., Moulin S., Peltier G., Li-Beisson Y., Beisson F., Sorigué D. Microbial photoproduction of *n*-heptane. Biofuel Research Journal 47 (2025) 2470-2486. DOI: 10.18331/BRJ2025.12.3.3.

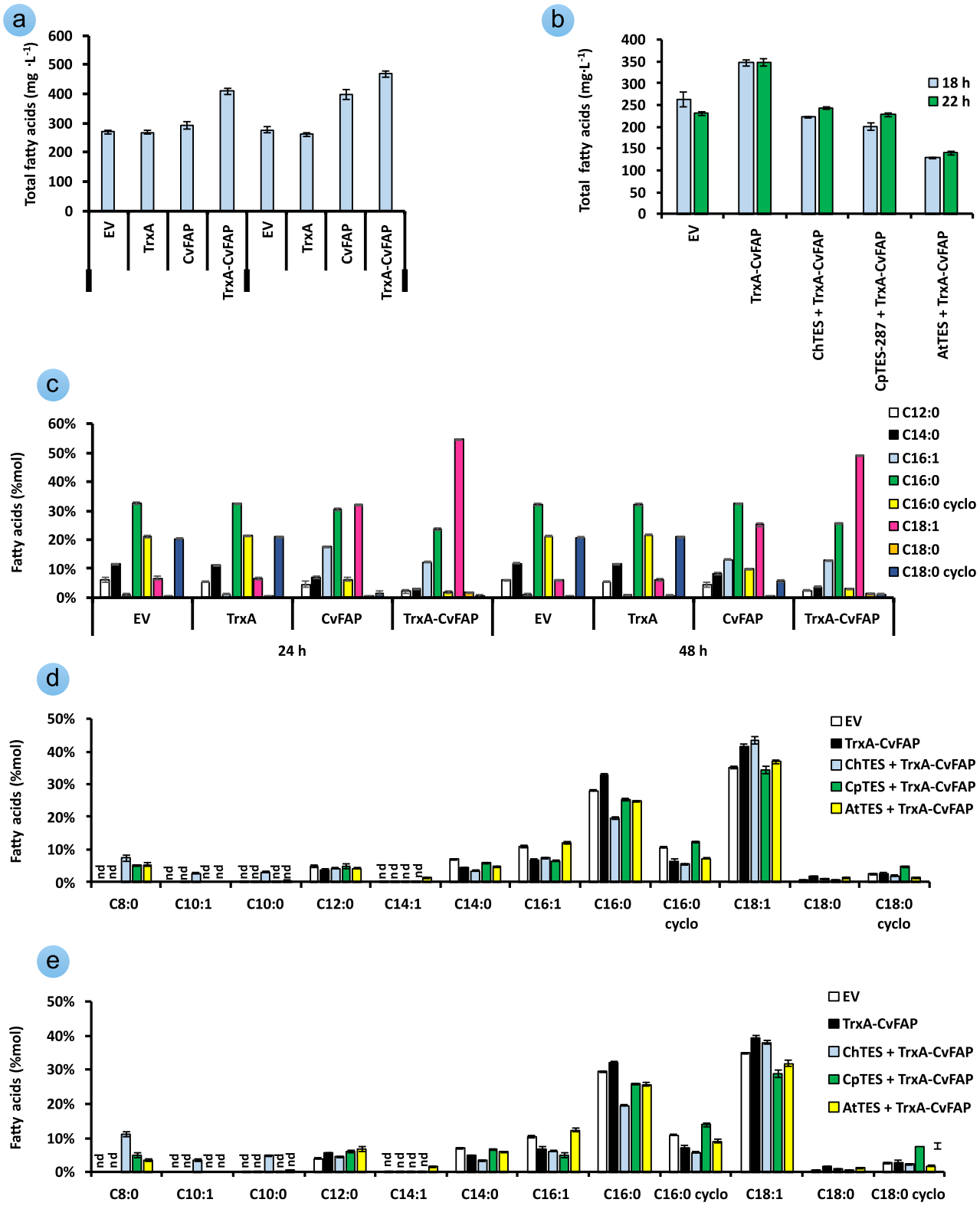

Fig. S2. Fatty acid profiles in *E. coli* expressing *Cv*FAP ± C8TESs. a) Total fatty acid content in strains expressing *Cv*FAP ± TrxA fusion, after 24- to 48-h of induction with 0.5mM IPTG under blue light (100 µmol photons·m^{-2}·s^{-1}). **b)** Total fatty acid content in *strains* co-expressing TrxA-*Cv*FAP with various C8TESs using pDawn plasmid, before and after 4 h of blue light (300 µmol photons·m^{-2}·s^{-1}). **c)** Distribution of fatty acids in strains expressing *Cv*FAP ± TrxA fusion. **d–e)** Fatty acid composition in different C8TESs and *Cv*FAP co-expressing strains measured (**d**) before and (**e**) after 4 h of blue light (300 µmol photons·m^{-2}·s^{-1}). An EV strain serves as a control. Error bars represent the standard error (n=3). 'nd' = not detected. C16:0 cyclo = methylenehexadecanoic acid, C18:0 cyclo = methyleneoctadecanoic acid.

Please cite this article as: Baca-Porcel Á., Samire P.P., Legeret B., Auroy-Tarrago P., Veillet F., Giacalone C., Cuine S., Moulin S., Peltier G., Li-Beisson Y., Beisson F., Sorigué D. Microbial photoproduction of *n*-heptane. Biofuel Research Journal 47 (2025) 2470-2486. DOI: 10.18331/BRJ2025.12.3.3.

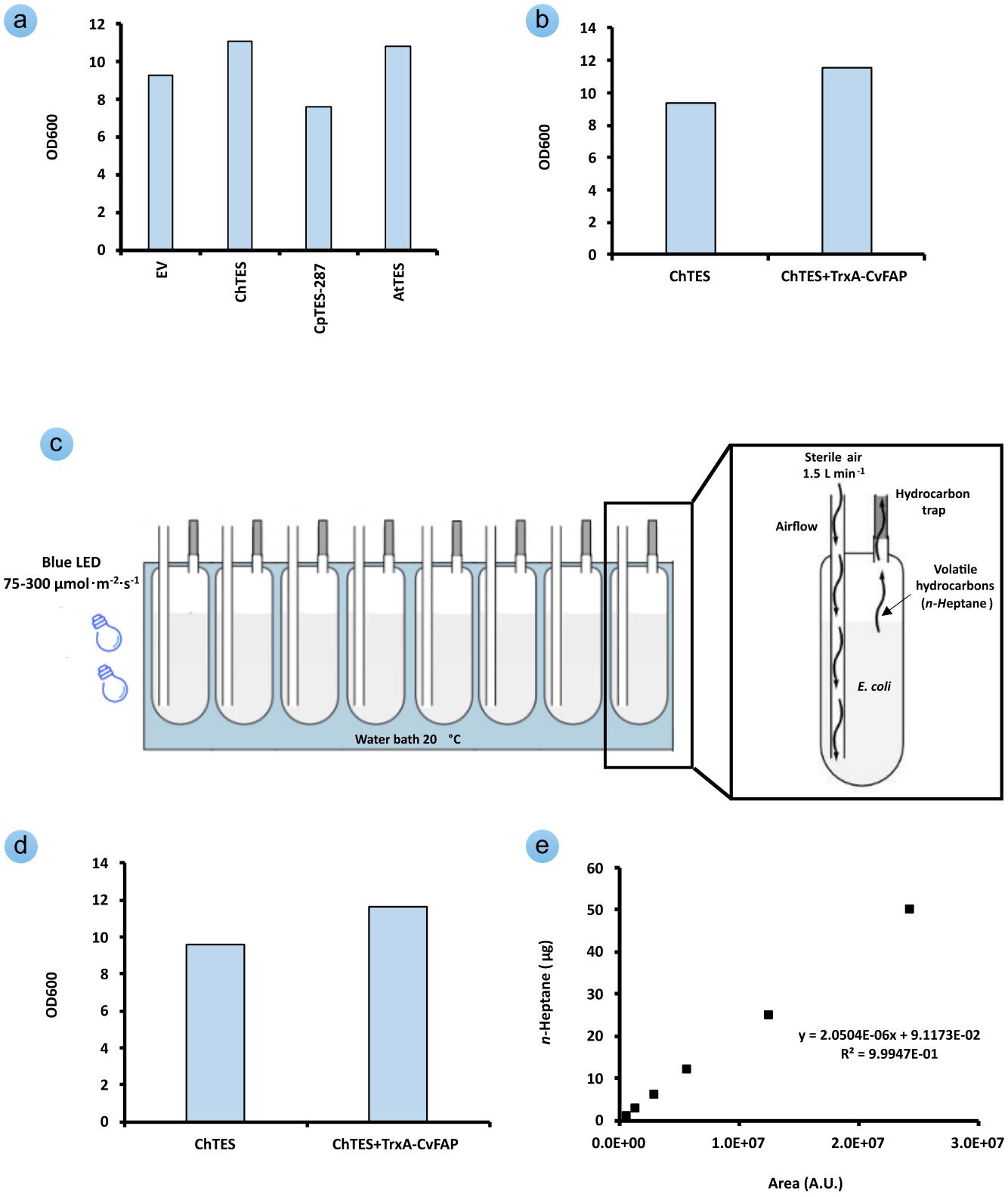

Fig. S3. Photoproduction of *n*-Heptane in a 100-mL photobioreactor using *Cv*FAP and *Ch*TES strains. a–b) Optical density measurements of *E. coli* strains expressing **(a)** various C8TESs and **(b)** co-expressing *Ch*TES ± *Cv*FAP after 18 h induction 0.2 µmol photons·m^{-2}·s^{-1} of blue light. **c)** Schematic representation of the 100 mL photobioreactor with controlled light, temperature, airflow, and volatile capture *via* a charcoal liner. **d)** Optical density of strains co-expressing *Ch*TES with *Cv*FAP or *Ch*TES only, after 18 h induction under 0.2 µmol photons·m^{-2}·s^{-1} of blue light before photobioreactor assays. **e)** External standard curve for *n*-heptane generated by adding increased *n*-heptane amounts to the activated charcoal liners.

Please cite this article as: Baca-Porcel Á., Samire P.P., Legeret B., Auroy-Tarrago P., Veillet F., Giacalone C., Cuine S., Moulin S., Peltier G., Li-Beisson Y., Beisson F., Sorigué D. Microbial photoproduction of *n*-heptane. Biofuel Research Journal 47 (2025) 2470-2486. DOI: 10.18331/BRJ2025.12.3.3.